

1 **Drainage reorganization during mountain building in the river**
2 **system of the Eastern Cordillera of the Colombian Andes**

3

4 Lucía Struth[‡], Julien Babault, Antonio Teixell

5

6 Departament de Geologia, Universitat Autònoma de Barcelona, 08193 Bellaterra
7 (Barcelona), Spain.

8 [‡] Corresponding author. +34935811035/+34935811263, Lucia.Struth@gmail.com

9

10 **ABSTRACT**

11 The Eastern Cordillera of Colombia is a thick-skinned thrust-fold belt that is characterized
12 by two topographic domains: (1) the axial zone, a high altitude plateau (the Sabana de
13 Bogotá, 2500 m asl) with low local relief and dominated by longitudinal rivers, and (2) the
14 Cordillera flanks, where local relief exceeds 1000 m and transverse rivers dominate. On the
15 basis of an analysis of digital topography and river parameters combined with a review of
16 paleodrainage data, we show that the accumulation of shortening and crustal thickening
17 during the Andean orogeny triggered a process of fluvial reorganization in the Cordillera.
18 Owing to a progressive increase of the regional slope, the drainage network evolves from
19 longitudinal to transverse-dominated, a process that is still active at present. This study
20 provides the idea of progressive divide migration toward the inner part of the mountain belt,
21 by which the area of the Sabana de Bogotá plateau is decreasing, the flanks increase in
22 area, and ultimately transverse rivers will probably dominate the drainage of the Cordillera.

23

24 *Keywords:* drainage network; fluvial capture; drainage evolution; Eastern Cordillera of
25 Colombia

26 **1. Introduction**

27 In the internal, thickened, and uplifting parts of the orogens, rivers are expected to follow
28 the regional slope and flow perpendicular to the structural trend of mountain ranges, a
29 pattern always matched by numerical models of continental-scale surface processes (e.g.,
30 Koons, 1995; Kooi and Beaumont, 1996; Willett et al., 2001; Goren et al., 2014). However,
31 during mountain building, active folds and thrusts can deviate rivers from the regional slope
32 (e.g., Van der Beek et al., 2002). Conceptually, the ability or not of preexisting reaches to
33 incise uplifting structures controls the number of diversions, and by extension it determines
34 the drainage organization, a phenomenon confirmed by modeling (Koons, 1994, 1995;
35 Tomkin and Braun, 1999; Humphrey and Konrad, 2000; Champel, 2002; Van der Beek et
36 al., 2002; Sobel et al., 2003). Additional factors such as bedrock lithology determine spatial
37 changes in strength and erodibility, and climate may control changes in weathering and
38 discharge.

39 Babault et al. (2012) showed in the High Atlas Mountains of Morocco (a thrust-fold belt
40 formed by tectonic inversion of a continental rift) an evolution from early fold- and fault-
41 controlled longitudinal rivers to a transverse-dominated drainage network during mountain
42 building and crustal thickening in response to a progressive increase in regional slope. This
43 may be a common transient mechanism of fluvial network evolution in mountain belts
44 (Babault et al., 2013).

45 A fluvial capture implies changes in flow direction, that is, the flow/discharge of the
46 captured drainage basin (victim) is deviated toward the neighbor captor basin with higher
47 erosion potential caused by either higher local precipitation, erodibility, and/or slope (e.g.,
48 Brookfield, 1998). Unlike models that show progressive divide migration and small-scale
49 capture events during mountain building (Willett et al., 2001; Pelletier, 2004; Bonnet, 2009;
50 Castelltort et al., 2012; Perron et al., 2012; Goren et al., 2014), the model of evolution from
51 longitudinal- to transverse-dominated drainage network implies captures of large
52 longitudinal drainages and substantial modifications of sedimentary outflux into adjacent
53 basins, potentially influencing clastic systems and petroleum reservoirs. Captures of
54 longitudinal rivers by transverse rivers are episodic and initially localized, whereas the

55 integrated long-term effect of the episodic capture events may be a major drainage
56 reorganization as discussed in this work.

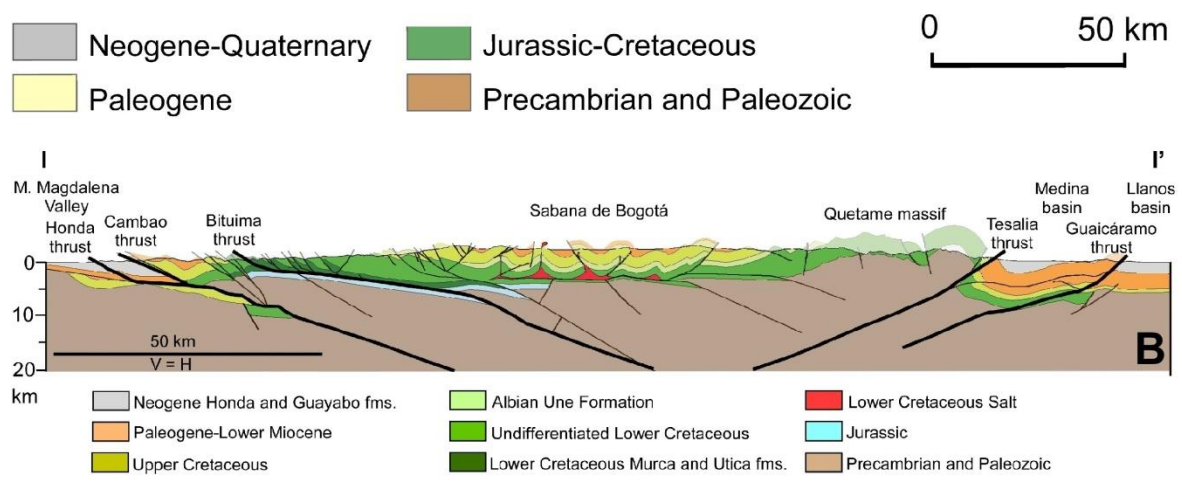
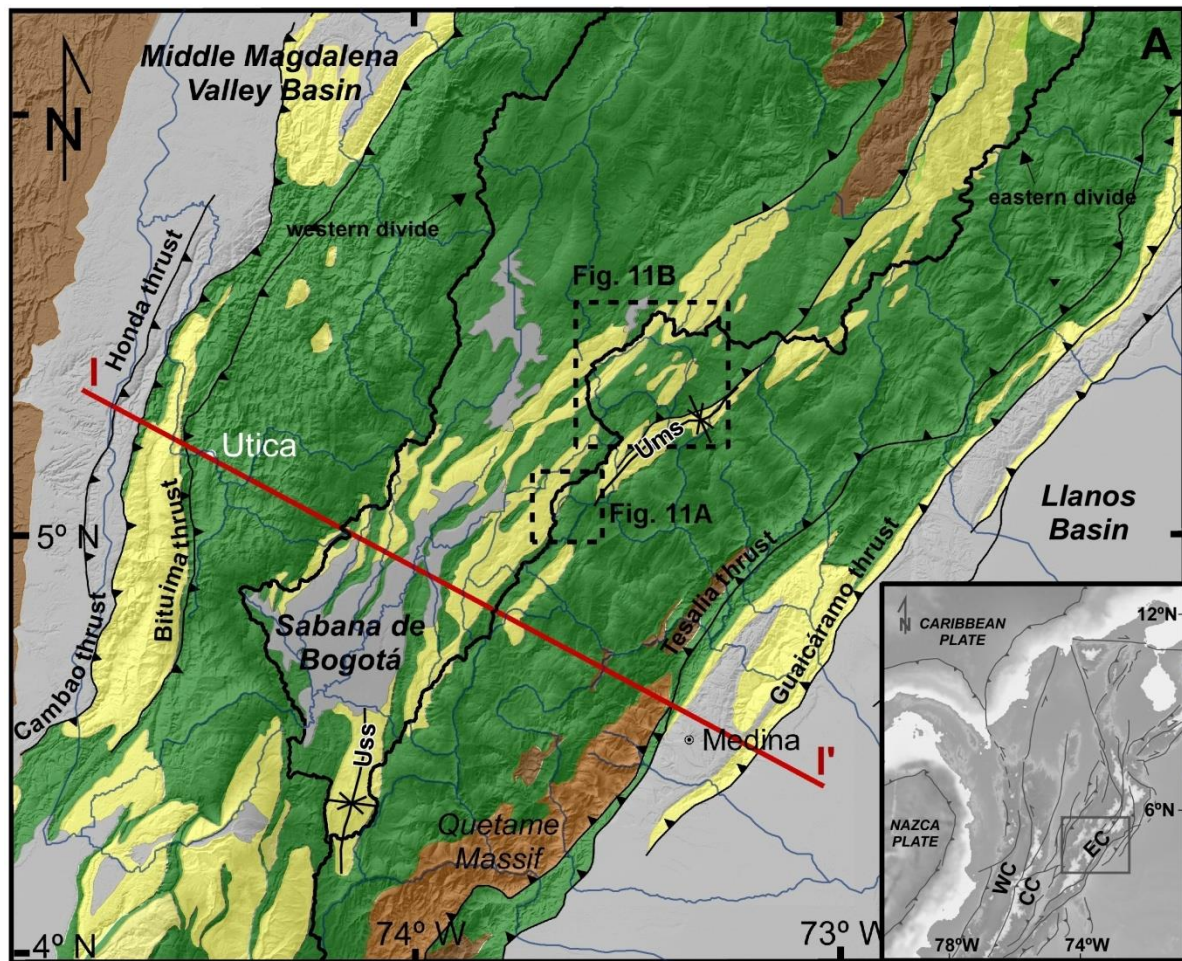
57 The aim of this study is to characterize the fluvial network and the drainage dynamics in
58 the central segment of the Eastern Cordillera of the Colombian Andes, as a case for
59 drainage reorganization. Like the High Atlas, the Eastern Cordillera of Colombia is an
60 example of a thrust-fold belt formed by the inversion of a former continental rift and shows
61 similarities in the fluvial network, with a high-elevation axial area dominated by low-energy
62 longitudinal rivers and with flanking belts of high-relief transverse valleys debouching into
63 the forelands. By means of field observations, morphometric analysis, and a review of
64 published palaeodrainage data, we first document that a longitudinal- to transverse-pattern
65 of fluvial evolution also applies to the Eastern Cordillera and then discuss a main
66 mechanism that may have enhanced drainage reorganization (and captures), together with
67 the potential implications for the downstream basin sediment supply.

68

69 **2. Regional setting**

70 *2.1. Geological setting*

71 The northern Andes in Colombia are divided into three belts: the Western, the Central,
72 and the Eastern Cordilleras. While the Western and Central Cordilleras are mainly
73 composed of crystalline rocks, including Precambrian to Paleozoic basement and Mesozoic
74 intrusives and ophiolites, the Eastern Cordillera is an inverted continental rift constituted by
75 a thick sequence of Mesozoic and Cenozoic sedimentary rocks (Julivert, 1970; Colleta et
76 al., 1990; Cooper et al., 1995) (Fig. 1A).



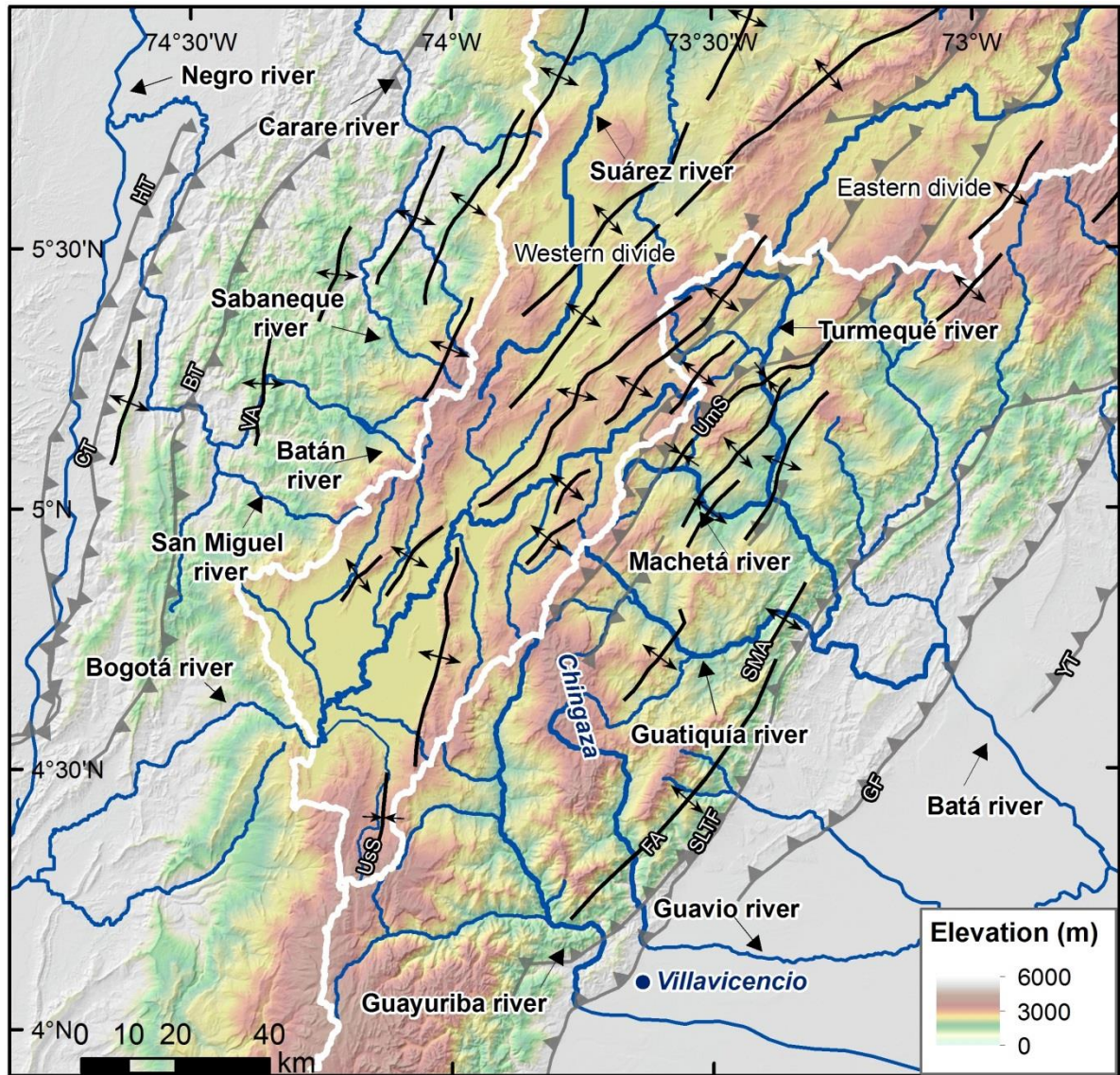
77

78 **Fig. 1.** (A) Geological sketch map of the study area in the Eastern Cordillera of Colombia.
 79 Thick black lines represent the western and eastern drainage divides, and thin blue lines
 80 correspond to the river network (modified from Babault et al., 2013). Inset shows a map of
 81 the northern Andes showing the location of the Eastern (EC), Central (CC), and Western
 82 (WC) Cordilleras of Colombia. (B) Structural cross section of the central part of the Eastern

83 Cordillera (location in Fig.1A). The main thrust faults in thick black lines are from west to
84 east the Honda, Cambao, Bituima, Tesalia (here including the Servitá-Lengupá and Tesalia
85 ss. faults) and Guaicáramo thrusts (modified from Teixell et al., 2015)

86 The Eastern Cordillera is a doubly-verging thrust system (Fig.1B) with a long
87 convergence history, but whose main episode of shortening and thickening began during
88 the Miocene as a response to the accretion of the Panama arc against the western margin
89 of Colombia (Duque-Caro, 1990; Kellogg and Vega, 1995; Rolon et al., 2004; Taboada et
90 al., 2000). Many of the thrust faults observed are derived from the reactivation of former
91 extensional faults of early Cretaceous age, belonging to the main episode of rifting in a
92 back-arc tectonic setting (Cooper et al., 1995; Mora et al., 2006, 2008; Tesón et al., 2013).
93 Since the mid-late Miocene, no major fault activity is recorded in the central or axial part of
94 the orogen; the main deformation was concentrated in the flanks (Mora et al., 2008;
95 Hermeston and Nemcok, 2013; Teixell et al., 2015). Evidence for active faulting along the
96 foothill thrust system, composed by the Servitá-Lengupá, Tesalia, Guaicáramo, and Yopal
97 thrusts, is provided by deformed terraces and fault scarps in Quaternary alluvial deposits
98 (Taboada et al., 2000; Mora et al., 2010; Hermeston and Nemcok, 2013; Veloza et al.,
99 2015).

100 From a topographic point of view (Fig. 2), the Eastern Cordillera can be divided into (I) a
101 plateau area of ~4300 km² at high altitude (~2500 m) in the axial zone, called the Sabana
102 de Bogotá; and (II) the Cordillera flanks and foothills, where deep incisions locally exceed
103 1000 m (e.g., middle-lower part of the Guayuriba River). The boundary between the plateau
104 and the flanks is defined by two main drainage divides.



105

106 **Fig. 2.** Main tectonic elements and rivers of the central part of Eastern Cordillera
 107 superimposed over digital topography. Thick white lines represent the western and eastern
 108 drainage divides between the axial plateau and flanks, and rivers are in blue (the main
 109 rivers highlighted by thicker lines). Grey barbed lines represent the main thrusts, and black
 110 lines represent the main folds. Rivers in the Sabana de Bogotá run parallel to the main
 111 folds, and rivers located in the flanks are transverse to the main tectonic structures. SLTF:
 112 Servitá-Lengupá, Tesalia faults; GF: Guaicáramo fault; YT: Yopal thrust; FA: Farallones
 113 anticline; SMA: Santa Maria anticline; VA: Villeta anticlinorium; BT: Bituima thrust; CT:
 114 Cambao thrust; HT: Honda thrust; UsS: Usme syncline; UmS: Umbita syncline.

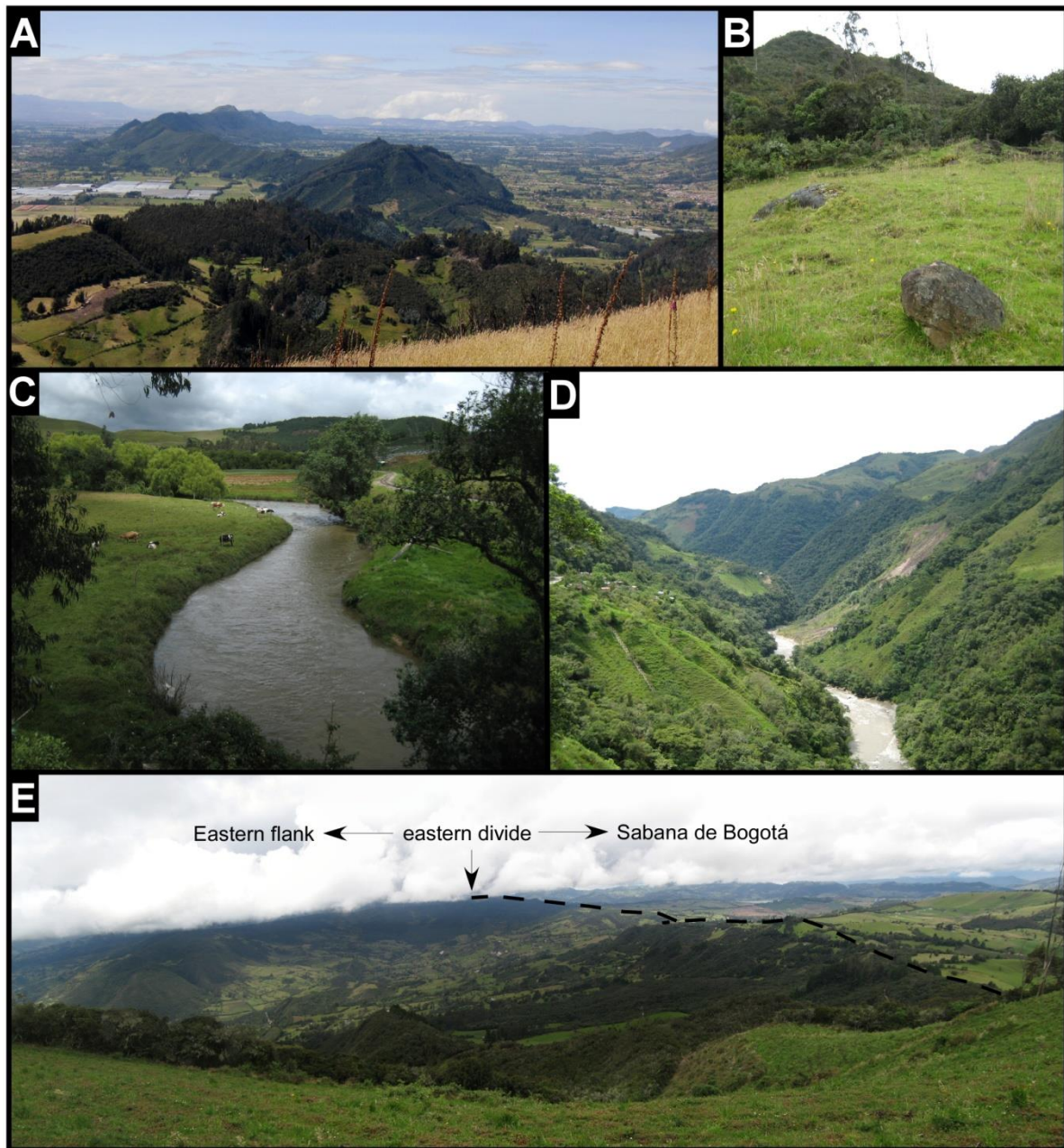
115 The Sabana de Bogotá is dominated by Cenozoic sandstone and shale formations with
116 upper Cretaceous sandstone outcrops in anticlinal cores (Fig.1). The flanks of the Cordillera
117 are characterized by lower and upper Cretaceous sandstone and shale formations and
118 isolated Precambrian to Paleozoic basement massifs. Despite the basement outcrops, no
119 overall difference exists in bedrock strength between the Sabana de Bogotá and the flanks,
120 as both are dominated at the surface by sandstone and shale formations. The Eastern
121 Cordillera is flanked on both sides by foreland basins dominated by Neogene and
122 Quaternary alluvial deposits that correspond to the middle Magdalena Valley basin in the
123 west and the Llanos basin in the east, at elevations of ~200-300 m asl.

124 Most of the tectonic shortening of the Eastern Cordillera is concentrated in the orogen
125 flanks, especially in the eastern margin (Fig. 1B). In the eastern thrust belt, basement rocks
126 are uplifted by thick-skinned thrust faults and exposed at the surface in the rugged
127 Quetame Massif (Toro et al., 2004; Mora et al., 2006, 2008). The western thrust belt does
128 not expose basement to the surface but is still characterized by large thrust displacements
129 (Gómez et al., 2003; Restrepo-Pace et al., 2004; Cortés et al., 2006). In contrast, the
130 interior of the Eastern Cordillera is constituted by the simple fold belt of the Sabana de
131 Bogotá (Figs. 1A, B) with low, rather homogeneous structural relief and without major
132 thrusting (e.g., Julivert, 1963; Mora et al., 2008; Teixell et al., 2015). As a whole, the
133 Eastern Cordillera was mostly uplifted by the major thrusts on the mountain flanks of the
134 belt (Fig. 1B).

135 The amount of orogenic shortening in the Cordillera is still in debate and depends on the
136 mode of thrusting adopted and on the role of the pre-orogenic extensional faults. Values of
137 150-200 km (up to 50%) of shortening have been calculated in thin-skinned models (e.g.,
138 Dengo and Covey, 1993; Roeder and Chamberlain, 1995), whereas smaller values of 70-
139 100 km (25-30%) are reported in thick-skinned models (e.g., Colletta et al., 1990; Cooper et
140 al., 1995; Tesón et al., 2013; Teixell et al., 2015).

141 *2.2. Fluvial drainage in the Eastern Cordillera*

142 Rivers in the Sabana de Bogotá run approximately NNE-SSW, parallel to fold axes, and
143 preferentially located in synclines (Fig. 2). Synclinal valleys are wide and flat, and ridges in
144 between correspond to anticline cores (Fig. 3A). The main river draining the plateau is the
145 Bogotá River, which ultimately incises into the western flank and drains to the Magdalena
146 River. The Bogotá River when draining in the plateau lengths 220 km; and its tributaries
147 flow to the SSW, parallel to the structural trend (Fig. 2). Rivers in the Sabana typically
148 show a general meandering pattern (Fig. 3C), gentle slopes, and low runoff velocity in
149 accordance with the smooth topography.



150

151 **Fig. 3.** (A) Field photograph of the Sabana de Bogotá showing the sandstone anticlinal
 152 ridge of the Chía Range (middle) and low slopes in adjacent synclinal areas. (B) Rock
 153 boulders product of a rockfall located on the eastern divide of the Cordillera, in the Machetá
 154 River capture zone (location in Fig. 9). (C) View of the longitudinal river Bogotá flowing in
 155 the plateau. (D) View of the transverse river Guayuriba in the eastern flank of the Cordillera
 156 with greater slopes and local relief, and common landslides in the hillslopes linked to the
 157 high slope angles. (E) Field image of the two topographic domains of the Eastern

158 Cordillera: the Sabana de Bogotá and the upstream part of the Machetá transverse river in
159 the eastern flank (field of view 4 km, view to the south).

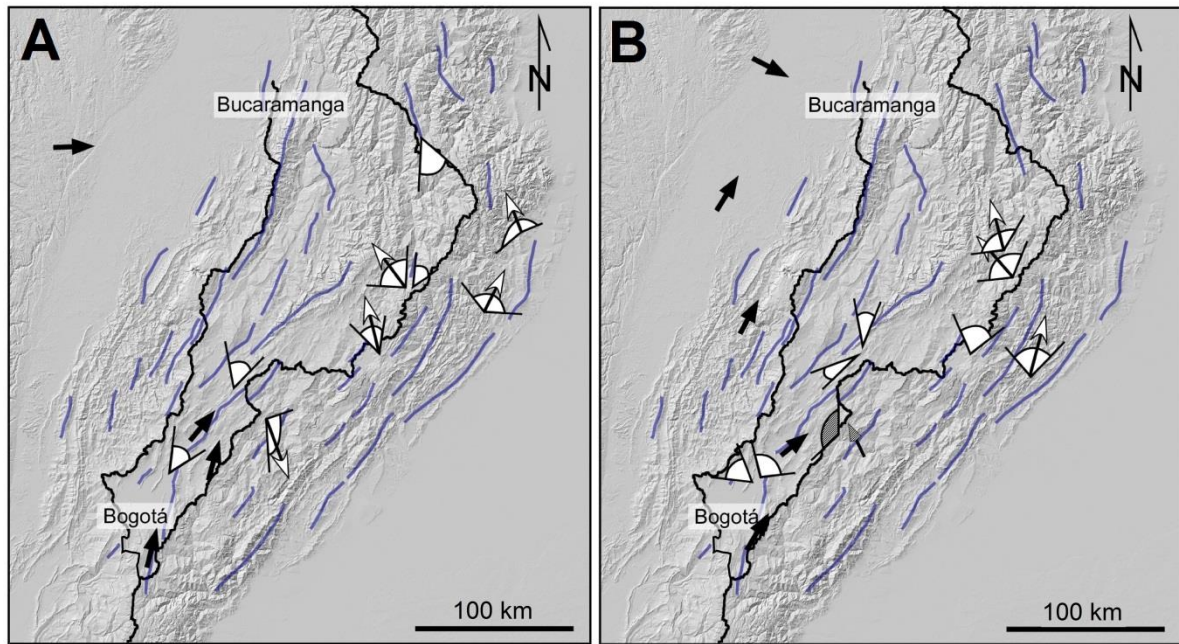
160 In the eastern flank of the Cordillera, the main rivers from south to north are Guayuriba
161 (Fig. 3D), Guatiquía, Guavio, and Batá rivers, draining to the Orinoco River in the Llanos
162 basin. These rivers range between 70 and 170 km long in the flank and flow perpendicular
163 to the structural grain, i.e., transverse to the trend of the Eastern Cordillera.

164 In the western flank of the Eastern Cordillera, the main rivers are the Río Negro and
165 Minero-Carare draining to the Magdalena River at the middle Magdalena Valley (108 ±46 m
166 of elevation in this region). These rivers are 150 and 110 km long, respectively, and flow
167 mainly in an E-W direction, transverse to the general trend of the Cordillera and
168 perpendicular to the main tectonic structures (Fig. 2). However, they also show sharp
169 changes in flow direction with longitudinal reaches separated by transverse reaches in the
170 medium and lower part of the western flank, displaying a gridiron-like drainage organization
171 which is common in fold-and-thrust belts (e.g., Gupta, 1997).

172 *2.2.1. Paleogene drainage in the Eastern Cordillera from paleocurrent data*

173 Paleocurrent and sediment provenance data of the early Cenozoic deposits of the
174 Eastern Cordillera indicate a western and southwestern sediment source and a drainage
175 network controlled by emerging folds and thrust sheets following a regional slope to the
176 NNE (Laverde et al., 1989; Cooper et al., 1995; Diaz and Serrano, 2001; Gómez et al.,
177 2005a; Bayona et al., 2008; Horton et al., 2010; Nie et al., 2010, 2012; Saylor et al., 2011;
178 Bande et al., 2012; Caballero et al., 2013; Silva et al., 2013).

179 In Paleocene-early Eocene times, there was a longitudinal drainage pattern (Fig. 4),
180 parallel to the structural grain (Brown et al., 1991; Gómez et al., 2005b,c; Bayona, 2008;
181 Bayona et al., 2008; Saylor et al., 2011; Mora et al., 2013; Silva et al., 2013). Paleocene
182 fluvial sediments in the Sabana de Bogotá region record paleocurrents to the NNE (Laverde
183 et al., 1989; Bayona, 2008; Bayona et al., 2008; Saylor et al., 2011).



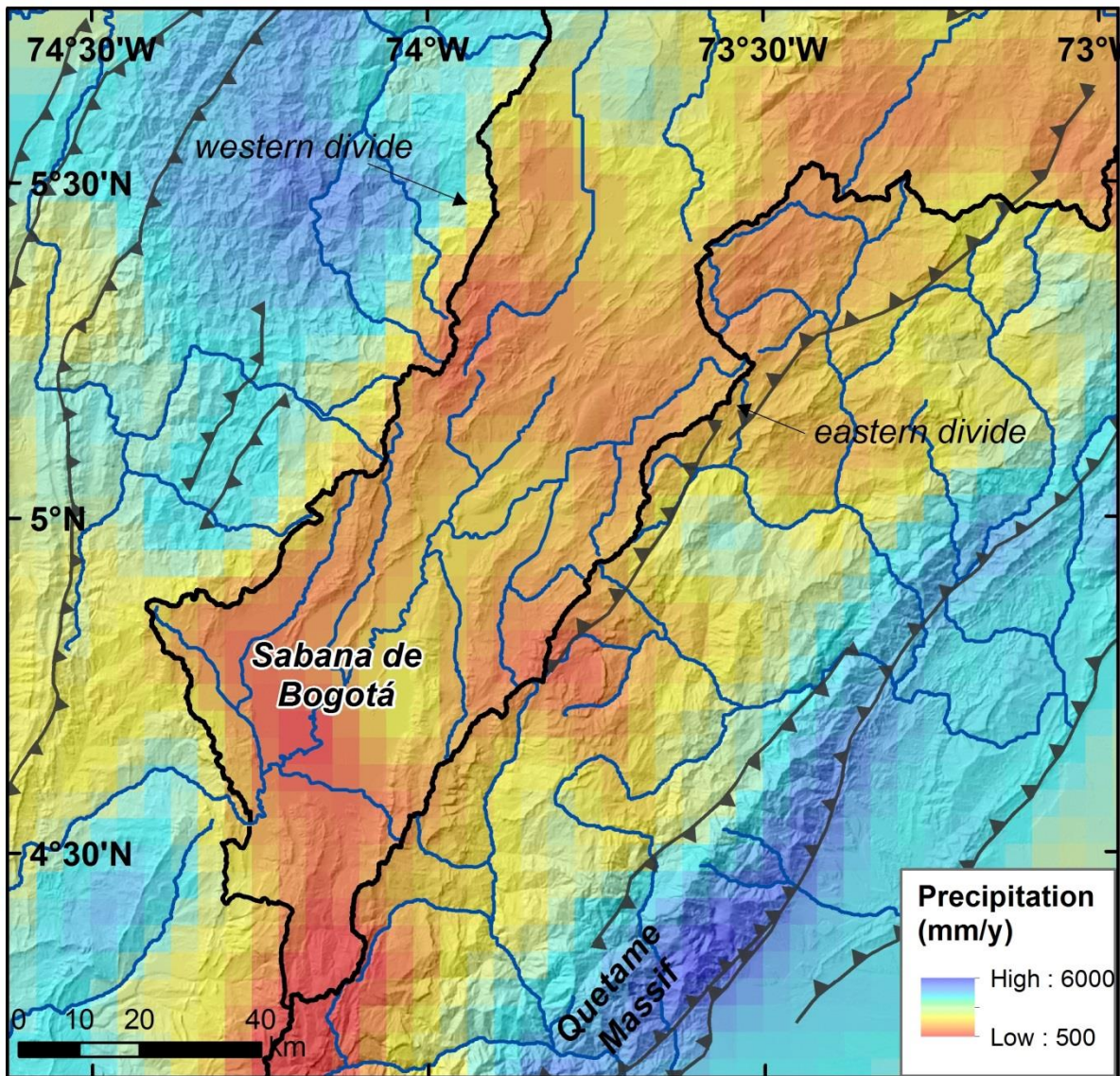
184
 185 **Fig. 4.** Summary of paleocurrent data from Paleocene (A) to Eocene (B) in the Eastern
 186 Cordillera compiled from Gómez et al. (2005b) (black arrows), Bayona et al. (2008) (white
 187 arrows), and Bayona (2008) (line-filled arrows).

188 The late Eocene-Oligocene still records a mean northward drainage in the current
 189 Sabana de Bogotá area and in the Magdalena Valley (Diaz and Serrano, 2001; Gómez et
 190 al., 2005a; Silva et al., 2013). In the late Oligocene to mid-Miocene interval, important
 191 changes occurred in the middle Magdalena Valley basin (MMVB): owing to deformation in
 192 the northern part of the basin, the base level started to rise and forced rivers to divert
 193 toward the Llanos Basin across the Eastern Cordillera (Gómez et al., 2005a,b). During the
 194 mid-late and late Miocene, the MMVB paleodrainage returned to the north in relation with
 195 continued rising of the Cordillera. In the eastern foreland of the Cordillera, a transverse,
 196 eastward paleocurrent direction is observed in the entire Miocene succession (Parra et al.,
 197 2010).

198
 199 **2.3. Summary of climate features**

200 Climate can be a major control on the evolution of drainage network (e.g., Schumm,
 201 1979; Bull, 1991; Whitfield and Harvey, 2012). A mean annual precipitation map (Fig. 5)

202 was compiled for the years 1998-2009 using TRMM data (Bookhagen and Strecker, 2008)
203 following the methodology of Bookhagen and Burbank (2010).



204
205 **Fig. 5.** Precipitation map of the Eastern Cordillera of Colombia compiled for the years 1998-
206 2009 (after Bookhagen and Strecker, 2008).

207 The map shows a strong gradient of precipitation in the vicinity of the western divide, by
208 which rainfall increases markedly in the western flank of the Cordillera. In contrast, a similar
209 gradient is not observed across the eastern divide, as the distribution of annual precipitation
210 is approximately homogeneous in the plateau and upper eastern flank. Precipitation is
211 higher in the eastern foothills and Quetame Massif.

212 The Sabana de Bogotá presents a sparse record of glaciation during the last 50 ka at
213 altitudes higher than 3500 m (Helmens, 1988, 1990; Helmens and Kuhry, 1995; Helmens et
214 al., 1997). On the basis of moraine deposits, glaciers are described as very small and
215 poorly developed valley glaciers or ice caps, ranging from 0.5 to 8 km² and were
216 deglaciated at ca. 12.5 ka (Helmens, 2004). U-shaped valley forms have never been
217 reported (Mark and Helmens, 2005).

218 *2.4. Summary of the deformation and uplift history of the Eastern Cordillera*

219 During the late Cretaceous and early Tertiary, the Eastern Cordillera was the foreland
220 basin system of the Central Cordillera (Cooper et al., 1995; Gómez et al., 2005a).
221 Progressive growth of the Eastern Cordillera structures since the late Maastrichtian or early
222 Paleogene disrupted and compartmentalized the foreland basin and ultimately subdivided it
223 into the Magdalena Valley and the Llanos basins (Gómez et al., 2003; Parra et al., 2009a,b;
224 Horton et al., 2010; Mora et al., 2013).

225 Based on subsidence and exhumation analysis (Parra et al., 2009a,b; Mora et al., 2010)
226 and detrital sediment provenance (Horton et al., 2010), the main emergence of the major
227 thrust faults in the flanks of the Eastern Cordillera started during late Oligocene to early
228 Miocene times. The disappearance of Meso-Cenozoic detrital zircons (which indicate a
229 Central Cordillera provenance) in the eastern foothills (Horton et al., 2010) indicates that
230 the Eastern Cordillera had already become an effective topographic barrier that separated
231 the Central Cordillera from the Llanos basin by the mid-late Miocene. This is marked by a
232 contemporaneous conglomeratic influx of the Honda and Guayabo formations (upper
233 Miocene to Pliocene) into the middle Magdalena Valley and Llanos basins (Hoorn et al.,
234 1995; Gómez et al., 2003; Parra et al., 2009a).

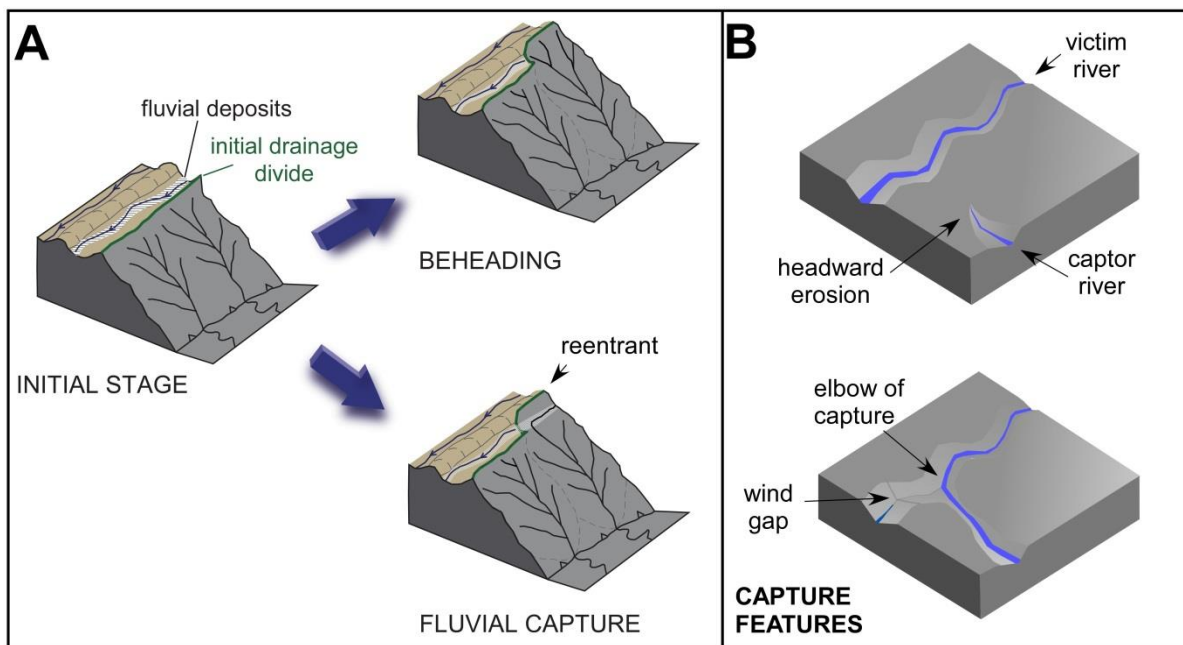
235 After a sedimentary hiatus that comprises most of the Oligocene and Miocene, the
236 Sabana de Bogotá accumulated ca. 600 m of fluviolacustrine deposits (Tilatá and Sabana
237 formations; Julivert, 1963; Andriessen et al., 1993; Torres et al., 2005), which partially filled

238 synclinal depressions and contributed to smooth the relief of the plateau as we see it today.
239 In spite of this, Van der Hammen et al. (1973) and Hooghiemstra et al. (2006) inferred low
240 altitudes for the Sabana until the late Miocene and a rapid surface uplift of 1500 ± 500 m
241 between 6 and 3 Ma ago, based on the palynological content of the late Neogene deposits
242 using the nearest living relatives method. However, these data may not be reliable enough
243 because Gregory-Wodzicki (2000) reported errors in paleoaltimetry estimates for the Andes
244 of ± 1500 m, implying that the proposed paleoelevation changes of the Sabana de Bogotá
245 may not be accurately resolved by the nearest living relatives method. For this reason, a
246 continuous crustal thickening and surface uplift since the onset of mountain building is not
247 discarded (Babault et al., 2013), as shortening was accumulating in a progressive way
248 (e.g., Moreno et al., 2013; Teixell et al., 2015) and explains the current high elevation of
249 the Eastern Cordillera.

250 **3. Digital topographic analysis**

251 Comparison of the paleodrainage data summarized above and the present-day fluvial
252 network of the Eastern Cordillera of Colombia suggests that drainage has experienced a
253 process of reorganization over geologic time. We undertook an analysis of the spatial
254 distribution of the local and mean slopes, of the drainage network organization, and of the
255 longitudinal profiles of the main rivers of the Cordillera with the aim of characterizing the
256 river dynamics and the signal of reorganization in the current network. According to Bishop
257 (1995), drainage rearrangement in mountain belts can be produced by beheading during
258 progressive divide migration and by discrete events of capture, which are mechanisms of
259 drainage expansion that result from headward erosion (Fig. 6A) The beheading process
260 results in the nonpreservation of early drainages, and thus capture elbows (sharp changes
261 in the river channel direction) and wind gaps (dry valleys with fluvial deposits) in the divide
262 are not preserved. However, low-elevation zones (anomalous depressions) in the
263 topographic profile of a divide may be the topographic expression of the migration of a
264 divide originally located at the crest and later reaching the bottom of an adjacent valley, as

265 reproduced in numerical models (e.g., Willett et al., 2001). Stream capture (piracy) can be
 266 identified by distinctive geomorphic features (e.g., Fig. 6B). These include the preservation
 267 of the early lines of the drainage network, elbows, and knickpoints (Small, 1978; Bishop,
 268 1995). Elbows and knickpoints cannot be used separately as a diagnostic for captures
 269 because changes in rock uplift and river diversion may also produce them. Other features
 270 potentially indicating capture events are hanging depressions (wind gaps) or discrete jumps
 271 (or reentrants) of a drainage divide, but they are seldom preserved in rapidly eroding
 272 settings like active orogenic belts (e.g., Clark et al., 2004; Prince et al., 2011; Brocard et al.,
 273 2012). Wind gaps correspond to segments of captured rivers where water no longer flows
 274 and show a width that is impossible to relate with the actual basin drainage area upstream
 275 (suggesting that they were created in past times with larger drainage areas). Stratigraphic
 276 evidence for captures include abandoned river terrace tracts and the existence of fluvial
 277 sediments with larger grain size than the current channel can transport or with lithologies
 278 linked to source areas that are now disconnected from the basin.



279
 280 **Fig. 6.** (A) Diagram showing the process of beheading and fluvial capture from the same
 281 initial stage. (B) Fluvial capture processes preserve the initial drainage lines and produce
 282 elbows and fluvial deposits in the divide (wind gap). These features do not occur in
 283 beheading.

284 **3.1. Methods**

285 In this study we analyzed the topography in the search of geomorphologic evidence for
286 divide migration and captures as previously mentioned. Beheading and stream captures
287 occur if disequilibrium of erosion exists between two catchments. We highlighted potential
288 disequilibrium of erosion by quantifying morphological differences between the axial plateau
289 of the Sabana de Bogotá and the steep Cordillera flanks between latitudes 5°30'N and
290 4°10'N (Fig. 2). We used the 90-m-resolution digital elevation model (DEM) SRTM90v4
291 (Jarvis et al., 2008) in the analysis. However, in areas where the fluvial channel is narrow
292 (<90 m), the SRTM90 DEM leads to overestimated elevations in gorges, providing wrong
293 data for river parameter extraction. Such errors were corrected using elevations from
294 Instituto Geográfico Agustín Codazzi (IGAC) 1:100,000 topographic maps and then
295 modifying the raster elevation matrix (DEM) pixel by pixel. Morphometric analysis and
296 calculation of the geomorphologic parameters described in the following sections was
297 carried out by using the D8 flow routine (eight-flow direction matrix; O'Callaghan and Mark,
298 1984; Tarboton, 1997; Mudd et al., 2014).

299 We compared the current drainage network geometry with the regional slope obtained
300 by calculating the local slopes of the mean elevations. The mean elevations have been
301 calculated with a moving window of 30 km of diameter. We compared the frequencies of
302 elevations, the local slopes, and the channel slopes between the plateau and the western
303 and eastern flanks of the Cordillera to highlight their topographic difference. In the
304 supplementary data we provide longitudinal river profiles of the main rivers draining the
305 Sabana de Bogotá and the Cordillera flanks.

306 River erosion depends at least on bedrock erodibility, water flow, and slope (e.g.,
307 Howard and Kerby, 1983). Analysis of slope-area relationships is often used to reveal
308 spatial trends of erosion and/or rock uplift in channel networks by the mean of the channel
309 steepness index or K_{sn} (e.g., Kirby and Whipple, 2001; Kirby, 2003; Snyder et al., 2003;
310 Wobus et al., 2006; DiBiase et al., 2010). However, scatters in local slope data in regions of
311 noisy and low-resolution DEM such as the Eastern Cordillera prevent accurate estimates of

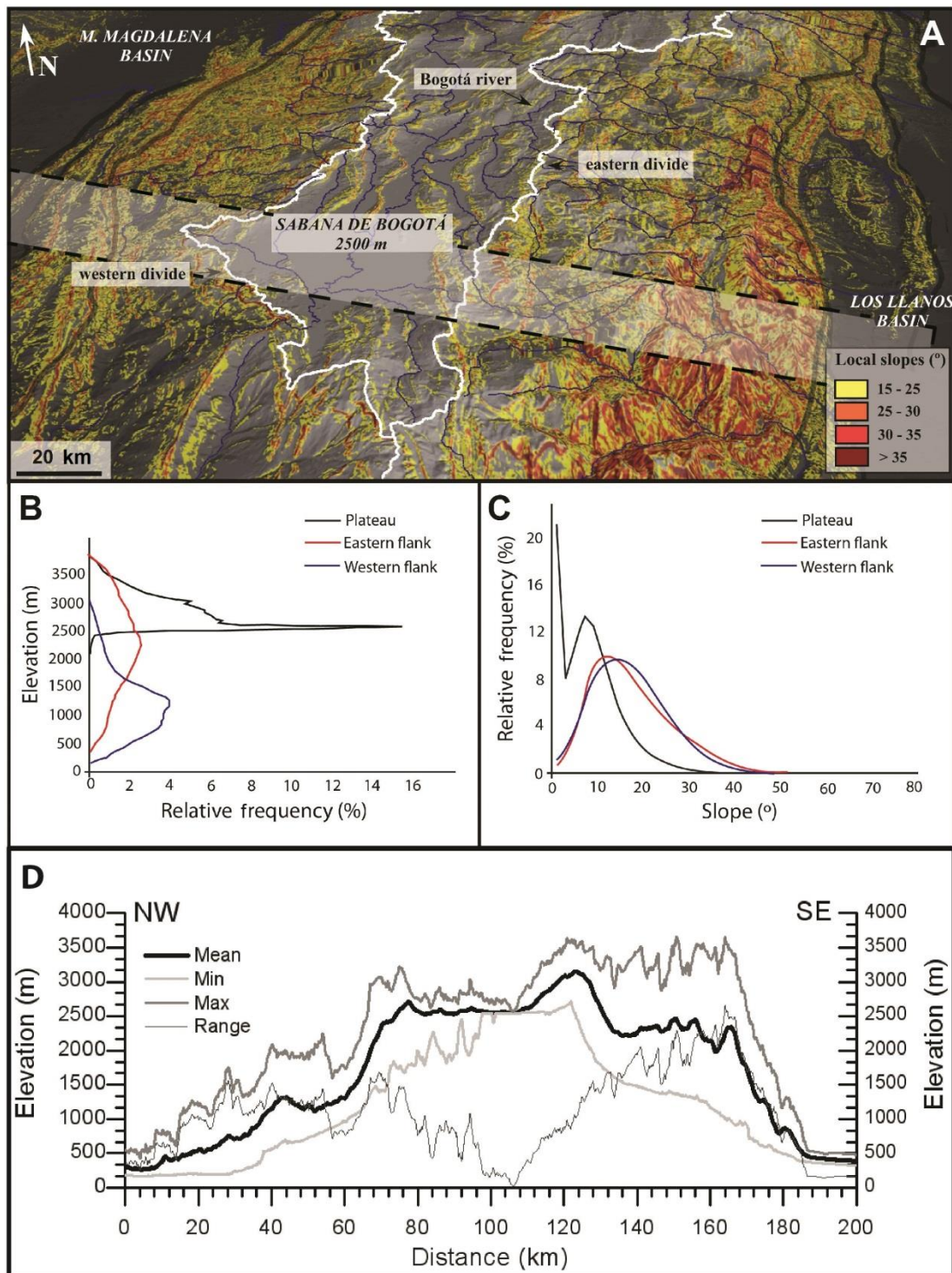
312 normalized channel steepnesses. Therefore, for the measurement of the normalized
313 channel slopes we preferred an alternative methodology, the χ (chi) gradient (Mx)
314 approach, where the river profile elevation (instead of the slope data) is the dependent
315 variable that is plotted against the integral of the drainage area (χ) as the independent
316 variable, giving more accurate results (Perron and Royden, 2013; Mudd et al., 2014). The
317 value of the channel slope in χ -elevation space (Mx) depends on the concavity, and we
318 determined the best concavity with AICc-collinearity tests and χ -plots following the method
319 developed by Mudd et al. (2014). Assuming that rock uplift is balanced by erosion (steady-
320 state condition) and that uplift, erosion, and erodibility are constant in time and space, the
321 stream power theory predicts that river profile will have a linear χ plot and Mx is
322 proportional to erosion rates (Royden and Perron, 2013; Mudd et al., 2014). However,
323 transient states where uplift rates change spatially or temporally can lead to piecewise
324 (stepped) channel profiles. In this case, we used the collinearity test to identify the
325 concavity (m/n ratio) for each river basin that best collapses the tributaries in χ -plots (Mudd
326 et al., 2014).

327 We generated topographic elevation profiles of the eastern and western main divides,
328 and we calculated their mean elevation using an adjacent-averaging smoothing method
329 (over 900 and 550 km distance for the eastern and western divide, respectively). Smoothing
330 with the adjacent-averaging method calculates the average of elevations around each point
331 and replaces the actual elevation of the point with the average value. The location of the
332 divide depressions (low-elevation segments) was compared with the geometry and
333 characteristics of the current drainage network. A fluvial capture leaves depressed zones or
334 gaps in the drainage divide where water does not actually flow (wind gaps). These
335 depressed zones can have fluvial sediments relict of the old fluvial drainage network.

336 3.2. *Analysis and results*

337 The differentiation between the topographic domains of the Eastern Cordillera is evidenced
338 by the results of the morphometric analysis. A first differentiation is based on
339 hypsometric and slope frequency curves (Fig.7). The plateau region shows a high
340 frequency in elevation around 2500 m, corresponding to the average elevation of the
341 Sabana plains (Figs. 7B and D). This region is also characterized by a high frequency
342 (21%) of slopes of $< 3^\circ$ and secondary maxima close to 8° (14%) (Fig. 7C). On the other
343 hand, the flanks of the Cordillera show a wider range of elevation. The eastern flank shows
344 the highest frequency values close to 2300 m, whereas in the western flank they are close
345 to 1300 m. The Cordillera flanks also show a higher local relief, with local slopes greater
346 than 10° . Greater local slope values ($>30^\circ$) are located in the external parts of the flanks
347 coinciding with the frontal fold-thrust structures (Servitá, Lengupá and Tesalia faults and
348 Farallones anticline in the eastern flank; Bituima fault and Villeta anticlinorium in the
349 western flank; Fig. 2).

350 The Sabana de Bogotá plateau shows a short range of elevation, giving a high frequency in
351 2500 m. The Cordillera flanks are characterized by a wider range of elevation values.

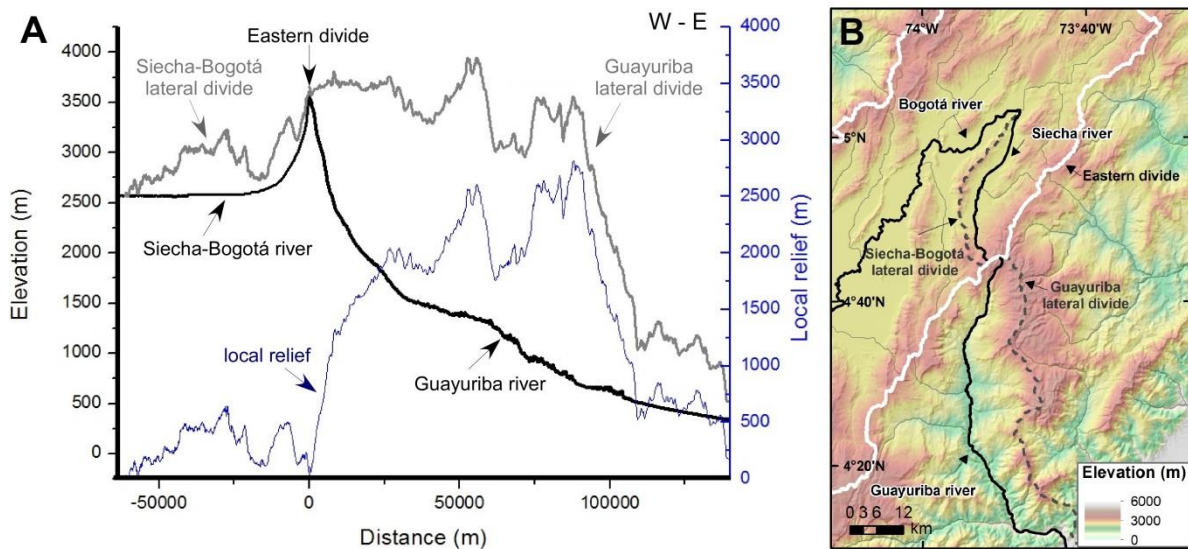


352

353 **Fig. 7.** (A) Oblique view of the Eastern Cordillera indicating local slopes (in colors). The
 354 transparent white band indicates the location of the 30-km swath used for the elevation
 355 profiles in (D). (B) Plot of the relative frequency of elevations that characterize each
 356 topographic domain defined for the Eastern Cordillera. (C) Plot of relative frequency of
 357 slopes in each domain. (D) Orogen-transverse topographic profiles of the Eastern Cordillera

358 along the swath indicated in (A), including maximum, minimum, and mean elevations and
359 the elevation range (difference between maximum and minimum).

360 The contrast between the plateau and the eastern flank is illustrated in Fig. 8, where we
361 plot the long profile of the Guayuriba River in the eastern flank and the profile of the Siecha-
362 Bogotá River in the plateau, including the projections of lateral divides and local relief for
363 each one. The plateau area, represented in Fig. 8 by the Siecha-Bogotá river, is
364 characterized by a low-elevation lateral divide and a very low local relief (500 m maximum).
365 In contrast, the Guayuriba basin, in the eastern flank, is characterized by a higher-elevation
366 lateral divide, as well as by a greater local relief (up to 2750 m).



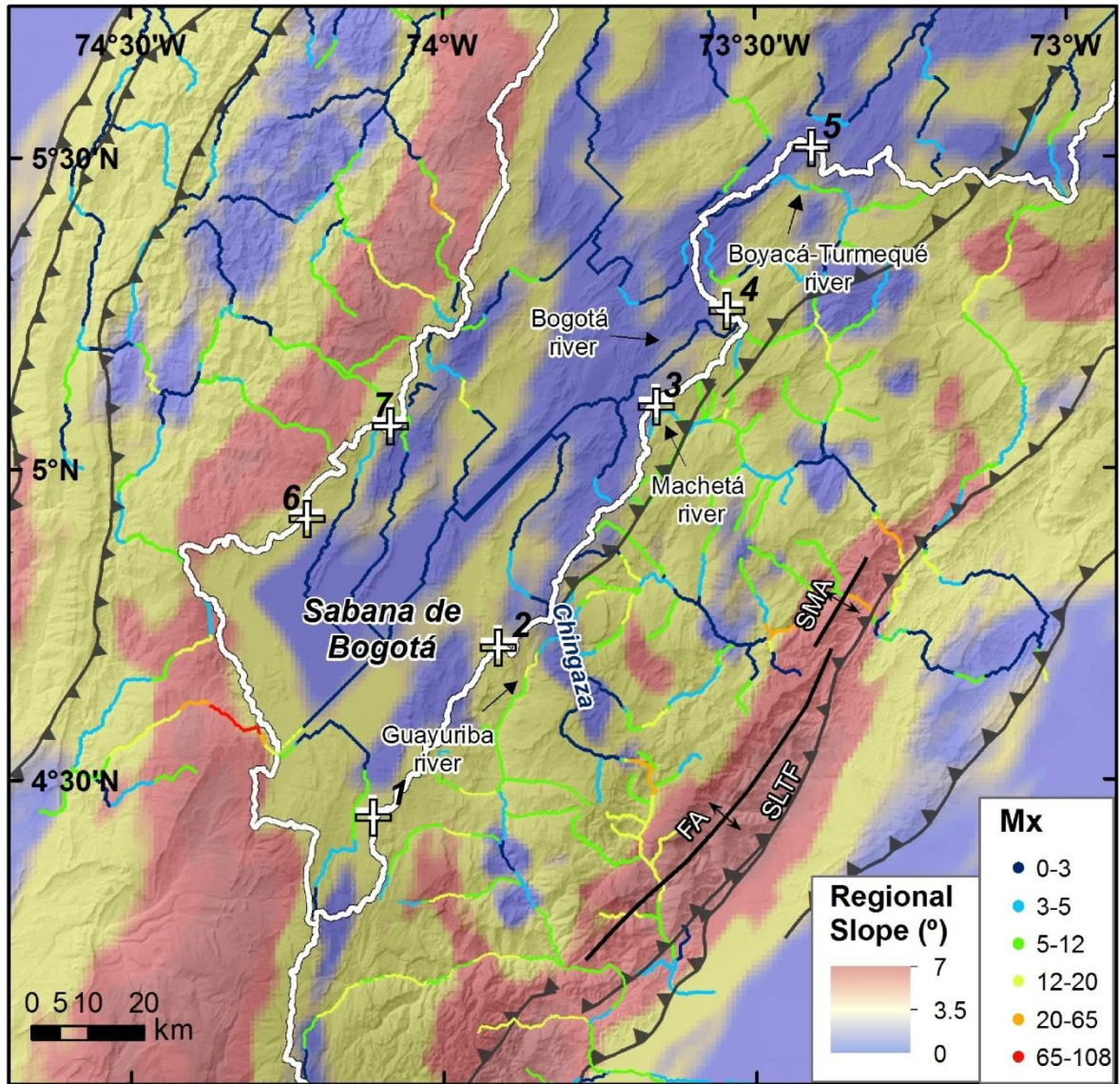
367
368 **Fig. 8.** (A) Longitudinal profiles of the Siecha-Bogotá (Sabana de Bogotá plateau) and
369 Guayuriba (eastern flank) rivers, compared with a projection of their lateral divides and the
370 local relief (difference between maximum and minimum elevations) between rivers and
371 divide ridges. (B) Location map of the rivers and divides shown in (A).

372 Mean regional slopes in the Eastern Cordillera illustrate that the Sabana de Bogotá
373 plateau is characterized by a very low mean regional slope of 1° (Fig. 9) and rivers follow
374 the main structures longitudinally. Rivers in the eastern flank follow the regional slope, that
375 is, to the east. The eastern flank shows greater mean slope values than the plateau, which

376 becomes greatest in the lower part of the flank (mean values of 2.5° and, 4.5° respectively;
377 Fig. 9). The western flank shows high values of regional slope (mean value of 4.5°)
378 immediately west of the western divide where the main rivers are also transverse.

379 Significant variations in channel slope (expressed by Mx , the slope in χ -elevation plots)
380 are not only observed between the Sabana and the flanks. Relevant variations in channel
381 slope occur either along the same river or between different rivers in each domain (see
382 supplementary data, SD1). The Mx values were calculated in function of the best concavity
383 for all basins analyzed. We found a 0.45 concavity as the best value based on the AICc-
384 collinearity test and χ -plots (see supplementary data, SD2 and SD3).

385 The map distribution of the Mx index of major rivers (Fig. 9) shows generally low values
386 (Mx 0-3) in the plateau area, coinciding with the lower regional slope and consistently with
387 the results of digital analysis of local slopes and with field observations: rivers in the plateau
388 show a meandering morphology (Fig. 3C) as well as lower slope and runoff velocity than
389 those in the flanks (Fig. 3D). The eastern flank shows Mx average values between 5 and
390 12, with peaks of 20-27. The greatest values are located in areas of recent tectonic uplift
391 (e.g., Farallones and Santa Maria anticlines in the eastern flank; Mora et al., 2008) or in
392 rivers with a drastic slope increase where they leave high-elevation, low-relief upstream
393 areas like the Chingaza region (see Fig. 2). The Mx values in the higher parts of the
394 western flank (bordering the divide), where rivers are transverse, range around 5-12, and
395 the Mx values decrease in the lower part of the flank where rivers are longitudinal (Mx 1-4).

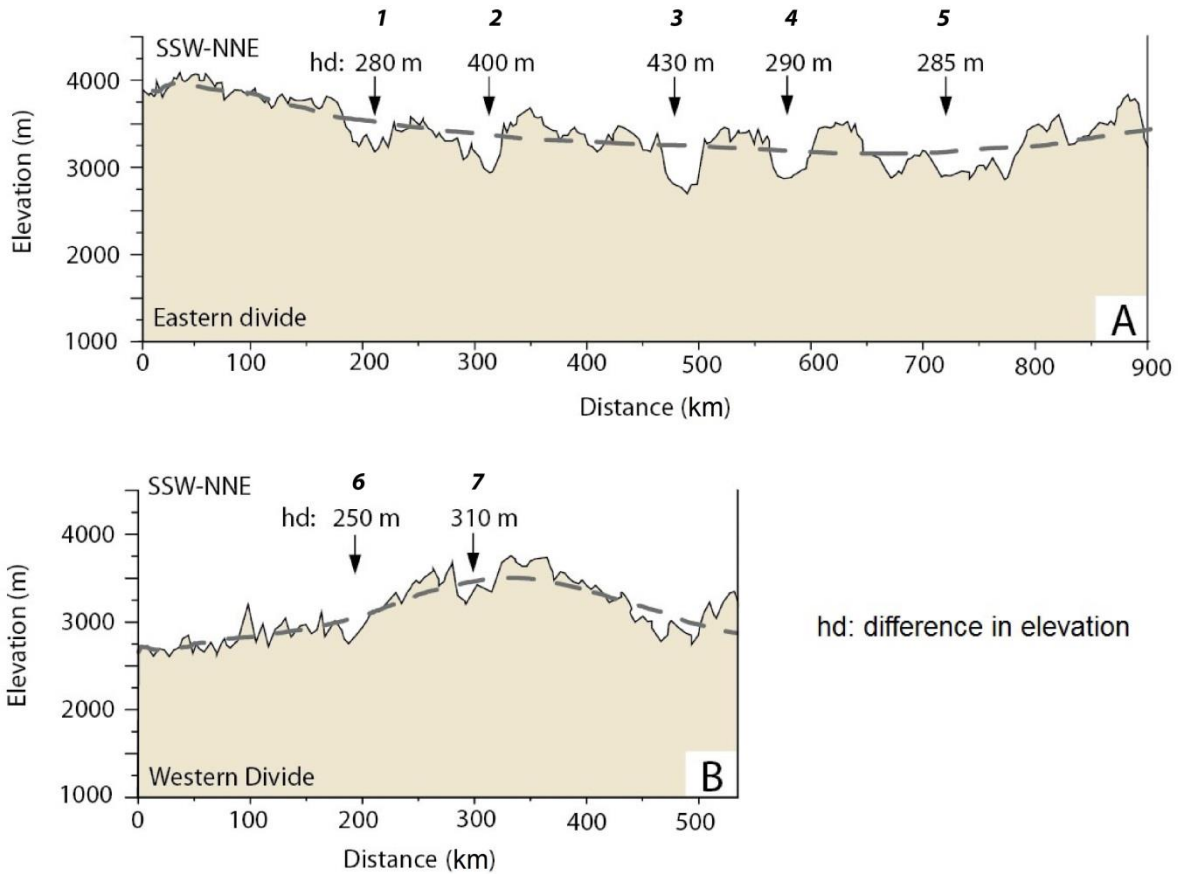


396

397 **Fig. 9.** Map of M_x (slope in χ -elevation plots) values for the analyzed rivers and regional
 398 slope ($^\circ$) calculated with a mobile window of 30 km diameter. The eastern and western
 399 divides are indicated by white lines. Note low M_x values in the Sabana de Bogotá and high
 400 values in the flanks of the Cordillera. Depressions in the divide ridges are indicated by white
 401 crosses and labeled with numbers from 1 to 7 (see text for discussion). FA: Farallones
 402 anticline; SMA: Santa Maria anticline; SLTF: Servitá-Lengupá-Tesalia fault.

403 Topographic profiles of the two drainage divides separating the axial plateau of the
 404 Sabana de Bogotá from the eastern and western flanks (Fig. 10) show a series of
 405 depressions (low-elevation segments in the divide) several hundreds of meters deep

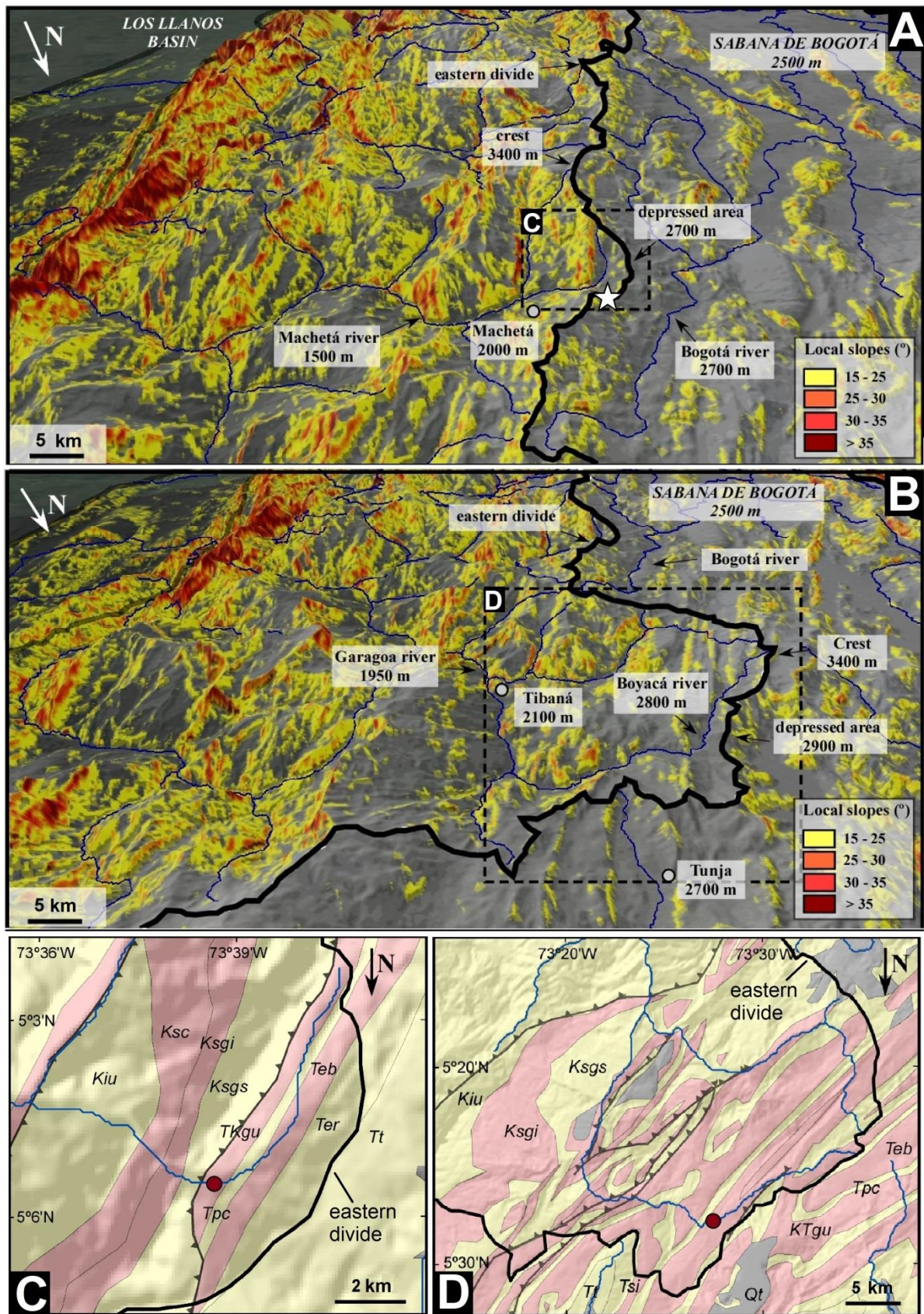
406 below the average elevation of the divide ridges. Depressions usually coincide with
 407 reentrants of the divide trace into the plateau (Figs. 9 and 10), i.e., segments of the divide
 408 that diverge from the main orientation and project toward the axial plateau of the orogen.



409
 410 **Fig. 10.** Profiles of the eastern (A) and western (B) drainage divides that bound the Sabana
 411 de Bogotá plateau showing the location of depressions (numbers in *italic* refer to Fig. 9).
 412 Additionally, we indicate the difference in elevation between the lower part of the divide
 413 (depressed area) and the mean elevation of the divide (dashed line).

414 An illustrative example of a divide depression is observed between the Machetá and
 415 Bogotá rivers (see Fig. 2 for location). In the headwater of the east-flowing Machetá River,
 416 the elevation low in the divide (2700 m) rises only 50 m above the longitudinal river in the
 417 Sabana (2750 m) (Fig. 11A). Local slopes are higher to the east of the divide (15°) than to
 418 the west in the plateau (5°) (Fig. 3E). Farther north, the depression in the eastern divide
 419 between the Boyacá-Turmequé and Bogotá rivers is only 80 m above the latter (Fig. 11B).

420 As in the case of the Machetá River, local slopes are higher to the east (20°) than in the
421 plateau (10°). In addition, the *Mx* of rivers is higher in the flanks than in the plateau (Fig.9),
422 in agreement with the distribution of local slopes. The depressions are associated with
423 elbow geometries with knickpoints in the downstream part of the longitudinal reach in the
424 flank rivers, and we do not observe spatial correlations with the trace of active faults nor
425 with easily erodible bedrock lithologies (Figs. 11C and D). Neither of these areas
426 correspond to zones of fold plunge (which could in principle provide low resistance to
427 incision and favor capture localization). This lack of correlation between divide depressions
428 or reentrants and tectonic structures or specific lithologies is observed all along the eastern
429 and western divides of the Eastern Cordillera.



430

431 **Fig. 11.** Local slope and lithology distribution at the Eastern Cordillera of Colombia. Note
 432 that they are oriented with North to the bottom of the page for a better appreciation of the

433 *topography and drainage. (A) Oblique view showing local slopes in the Eastern Cordillera.*
434 *A reentrant in the divide associated to a depressed area is indicated in Figs. 9 and 10,*
435 *testifying to processes of fluvial capture with a difference in elevation of 430 m between the*
436 *mean altitude of the divide and the bottom of the depression. The occurrence of rounded*
437 *rockfall deposits (Fig. 3B) is marked by a white star (see text for discussion). (B) Oblique*
438 *view indicating local slopes in the plateau and in the upstream part of the Boyacá-*
439 *Turmequé transverse river. The reentrant area is indicated in Fig. 9 and corresponds to a*
440 *depression in the elevation profile of the divide (see Fig. 10), with a difference in elevation*
441 *of 285 and 290 m. (C) and (D) Lithologic maps of the depressed divide in (A) and (B),*
442 *respectively, showing no lithologic or tectonic control on the divide depression and on its*
443 *trace. Red polygons are shale formations and yellow polygons sandstone formations. The*
444 *red circle shows the location of a knickpoint. Cretaceous and Tertiary sandstone*
445 *formations: Kiu (Une Fm), Ksgs (Guadalupe Superior Fm), Tpc (Cacho Fm), Ter (Regadera*
446 *Fm), Tt (Tilatá Fm), Tsi (Socha inferior Fm). Cretaceous and Tertiary shale formations: Ksc*
447 *(Chipaqué Fm), Ksgj (Guadalupe Inferior Fm), KTgu (Guaduas Fm), Teb (Bogotá Fm)*
448 *(modified from Toro et al., 2004; Parra et al., 2009b, Mora et al., 2010; and unpublished*
449 *maps by ICP-Ecopetrol).*

450 **3.3. River capture and evidence for drainage divide migration**

451 At present, the main rivers flowing in the Sabana de Bogotá plateau are longitudinal and
452 follow synclines constituted by Cenozoic strata, mostly terrestrial in origin. In the Cordillera
453 flanks, the main rivers are transverse to the chain and they are deeply incised across
454 Cretaceous and Paleogene folded series. As summarized above, during Paleocene-
455 Oligocene times, the drainage network was controlled by the emerging folds and thrusts
456 and followed a gentle regional slope to the NNE (Gómez et al., 2005a; Silva et al., 2013).

457 Incised transverse rivers that cut across the Paleogene folded series in the eastern flank
458 are evidence of a strong contrast between the current flow drainage organization and the
459 paleodrainage deduced from the Paleogene strata. The northern flow direction from

460 palaeocurrent data in these Paleogene series are now incised by an eastern transverse
461 flow. This is the case of the Tertiary Umbita and Usme synclines (Fig. 1). The Usme
462 syncline, with a N-S orientation parallel to the mean trend of the orogen, records an
463 Oligocene paleoflow in the same direction. Nevertheless, part of this syncline has been
464 captured by a river of the eastern flank and now drains to the east, which indicates a
465 migration of the main eastern divide toward the inner part of the Cordillera (the plateau)
466 after the Oligocene. The Umbita syncline records a western flow in Paleocene times (see
467 location in Figs. 1 and 4). This syncline is actually in the eastern flank and dominated by a
468 transverse drainage flowing to the east (Figs. 11A and C). Paleogene strata are not
469 preserved in the western flank of the Cordillera, and this line of evidence cannot be applied.

470 Captures usually leave gaps/depressions in drainage divides (e.g., Bishop, 1995). The
471 topographic profiles of the main divides of the Eastern Cordillera show low-elevation tracts
472 (Figs. 9 and 10). These depressed tracts coincide with map-view reentrants of the divide
473 trace toward the plateau, suggesting a drainage area transfer from the plateau to the
474 Cordillera flanks, as explained above. In addition, elbows with knickpoints at or above the
475 elbow can be observed in these areas (see Figs. 11C and D), and the channel slope map
476 (Mx values) (Fig. 9) also illustrates a strong topographic contrast across the main divides
477 separating the Sabana plateau from its flanks. On the other hand, rounded rockfall deposits
478 are locally found on the eastern divide into the Sabana plateau (Figs. 3B and 11A), where
479 none of the current debris flow corridors observed in the slopes of the surrounding peaks
480 lead to the rockfall deposit. This suggests that the missing crest that fed these boulders
481 must have been eroded away, indicating divide migration toward the plateau.

482 On the assumption that erosion balances the local base level fall, the Mx value relates to
483 the ratio between erosion rate and erodibility (Royden and Perron, 2013; Mudd et al.,
484 2014). Therefore, the high Mx values observed in the Eastern Cordillera flanks suggest
485 greater erosion rates than in the plateau. This may have favored the progressive divide
486 migration toward the plateau and captures of longitudinal rivers previously flowing in the

487 plateau by expanding transverse rivers in the flanks, thus providing an explanation for the
488 contrast between the Eocene paleodrainage organization recorded in the Usme and Umbita
489 synclines, and the current river network. We observe the same distribution of local slopes
490 and channel slopes (Mx) between the western flank and the axial plateau, suggesting a
491 similar migration in the western divide toward the centre of the Eastern Cordillera.

492 In summary, the depressions in the main divides, the occurrence in the flanks of
493 knickpoints in the upstream parts of the longitudinal river profiles (e.g., Chingaza area), the
494 existence of rock landslides with no source near the divide (Figs. 3B and 11), the
495 observation of elbows in the rivers of the eastern flank with knickpoints upstream, and the
496 contrast between the local slopes and the channel slopes of the main rivers support the
497 view that the drainage network of the Eastern Cordillera reorganizes by progressive divide
498 migration toward the inner part of the chain and by discrete events of capture. This is in
499 agreement with the reorganization inferred from the contrast between the palaeocurrent
500 data of the geological record and the present-day drainage network. The case of the
501 Umbita and Usme synclines (where youngest strata are Oligocene in age) indicates that in
502 those areas such reorganization did not start before the Miocene. As the main divides
503 converge toward the centre of the Eastern Cordillera, and given the scarcity of Cenozoic
504 strata in the Eastern Cordillera flanks, we cannot rule out that reorganization may have
505 started earlier in the external parts of the eastern and western flanks.

506 **4. Causes and implications of drainage reorganization**

507 *4.1. Mechanism causing drainage reorganization*

508 Our observations suggest that the drainage network in the Eastern Cordillera evolves
509 from longitudinal-dominated to transverse-dominated, with rivers turning into the direction of
510 the regional slope. The steep transverse rivers must have higher rates of incision than the
511 gentle longitudinal rivers in the plateau to expand their catchment. At least four potential
512 mechanisms that could explain differential erosion between the plateau rivers and rivers in
513 the flanks can be considered.

514 First, a gradient of precipitation perpendicular to the trend of an orogen can result in
515 divide migration toward the dry side, as has been observed in numerical models (e.g.,
516 Willett, 1999; Bonnet, 2009). Figure 5 shows the annual precipitation for the period 1998-
517 2009 in the Eastern Cordillera, where no precipitation gradient is observed across the
518 eastern main divide. On the basis of evidence as stable isotope geochemistry from fossil
519 and present-day growth bands in mollusks, from palynology, and from macroscopic
520 paleoflora, Mora et al. (2008) suggested that the influence of the erosion processes by
521 global climate change was negligible since the Pliocene in the region. The precipitation
522 pattern appears to have remained similar at least since middle Miocene time (Mora et al.,
523 2008, and references herein), coinciding with the early topographic growth causing the
524 topographic asymmetry of the orogen (Mora et al., 2008). Moreover, an eastward gradient
525 in moisture could not explain the similar contrast of morphology between the western flank
526 and the plateau. Therefore, the reorganization of longitudinal to transverse drainage may
527 not be attributed to an asymmetric precipitation pattern across the eastern divide.

528 Second, erodibility differences associated with lithological changes can explain spatial
529 variations in erosion rates (e.g., Safran et al., 2005) and can produce local changes in the
530 organization of drainage. In the Eastern Cordillera of Colombia, the depressions along the
531 main divides are not located on less-resistant lithologies, and they occur indistinctly over
532 shale or sandstone formations, from which we can conclude that the reorganization of the
533 drainage is not controlled by lithology.

534 Third, in some mountain settings at mid-latitudes, different intensity of glacial erosion by
535 valley or cirque glaciers may produce a divide migration toward the hillslopes receiving less
536 insolation (Brocklehurst and Whipple, 2002). The Eastern Cordillera of Colombia is close to
537 the equator so that the reorganization of drainage cannot be controlled by glacial erosion as
538 eastern and western slopes receive the same amount of insolation. Indeed, we see unlikely
539 that the small and poorly developed valley glaciers deduced for the Eastern Cordillera
540 during the Quaternary (Helmens, 2004) contributed to an important difference in erosion

541 between the flanks and the plateau, especially in view of the abundant fluvial
542 geomorphologic features that point for drainage reorganization.

543 Fourth, longitudinal drainage largely coincides with areas where the regional slopes are
544 low, whereas transverse rivers are related to higher regional slopes. The marked slope
545 contrast between the flanks and the plateau appears to be the sole factor responsible for
546 the higher erosional activity on the flanks. Consequently, we propose that the
547 reorganization of the drainage network in the Eastern Cordillera is the result of increased
548 regional slope. We interpret that the regional slope increase was acquired during orogenic
549 shortening and crustal thickening of the mountain belt. The slope contrast between the axial
550 plateau and the flanks associated with orogenic building promotes fluvial capture of the
551 initial longitudinal drainage area by the transverse drainage system. The longitudinal-to-
552 transverse drainage evolution thus deduced may represent a transient stage in mountain
553 building, as previously discussed for the High Atlas Mountains of Morocco by Babault et al.
554 (2012, 2013). Moreover, the occurrence of precipitation in the eastern flank will enhance
555 the eastern divide migration toward the central part of the Cordillera.

556 The dynamics of drainage network described here is currently active in the Eastern
557 Cordillera, and we can expect future captures to occur in areas where steep transverse
558 rivers flow close to low-gradient longitudinal rivers located in the plateau, especially if they
559 are separated by a low-elevation stretch of the main divide. As an illustrative example, the
560 Batán river in the western flank threatens to capture the Frío River in the Plateau (zone 7 in
561 Fig. 9).

562 *4.2. Implications for sediment supply into the adjacent basins*

563 Changes in the sediment supply, sedimentation rate and detrital composition are often
564 considered to be caused by climatic and/or tectonic variations (e.g., Molnar and England,
565 1990; Stokes et al., 2002; Allen, 2008). Drainage reorganization can exert, alternatively, a
566 control on the sedimentation rates (e.g., Mather, 2000; Stokes et al., 2002; Prince et al.,
567 2011; Antón et al., 2012; Willett et al., 2014). Capture processes involve sudden changes in

568 the drainage areas of the captor river and of the victim river. The captor river gains drainage
569 area and therefore the erosion rate increases connecting an elevated catchment to a lower
570 base level. The remnant drainage basin, the victim, experiences an erosion rate decrease
571 as it loses headwaters and drainage area. These variations must affect the clastic fluxes at
572 the outlets, and modify the spatial and temporal localization of the proximal clastic bodies at
573 the toe of the thrust front. Therefore, with the reorganization of the drainage network in the
574 Eastern Cordillera related to the increase of the regional slope, the transverse rivers located
575 in the flanks increased their drainage areas against the rivers located in the Sabana. In this
576 way, erosion of the captured areas may have enhanced sedimentation rates in the Llanos
577 and Magdalena basins.

578 Previous works interpreted the distribution of maximum sediment thickness of the late
579 Oligocene to Miocene Carbonera to Guayabo formations (which are coarse-clastic foreland
580 basin deposits derived from the Eastern Cordillera) as associated with the orogenic loads
581 (Parra et al., 2009a,b; Hermeston and Nemcok, 2013; Jimenez et al., 2013). We propose
582 that the migration of the orogenic load is not the only mechanism to explain sedimentation
583 rate increases, coarse-clastic inputs, and depocenter migration in the basins adjacent to the
584 Eastern Cordillera. The process of fluvial drainage reorganization in the source areas of the
585 mountain belt may have exerted an additional control.

586

587 **5. Conclusions**

588 The Eastern Cordillera of Colombia presents a clear differentiation into two topographic
589 domains: an axial plateau dominated by gentle longitudinal rivers, with low local relief and
590 local slopes, and the flanks with high local relief and slope dominated by steep transverse
591 rivers. These domains are separated by two main drainage divides in the eastern and
592 western sides of the Sabana de Bogotá plateau.

593 In the eastern flank of the Cordillera, the change in flow direction between the
594 Paleogene palaeodrainage toward the NNE, parallel to the early tectonic structures, and the

595 current drainage toward the SE, incising across folded Paleogene strata near the eastern
596 divide, argues for drainage reorganization. This work highlights the convenience of
597 morphological analysis to characterize drainage reorganization and supports models of
598 evolution of relief in mountain belts. Morphometric analysis and field observations show
599 depressions and map-view reentrants in the main divides, debris flow deposits with no
600 source near the divide, elbows with knickpoints upstream, and an evident contrast of the
601 local and river slopes across the divides. This evidence indicates that the drainage network
602 reorganizes by progressive divide migration toward the inner part of the chain by discrete
603 events of capture.

604 We interpret that fluvial reorganization from longitudinal to transverse-dominated
605 drainage in the Eastern Cordillera was triggered by the increase of the orogen regional
606 slope by the progressive accumulation of crustal shortening and thickening. This pattern of
607 drainage evolution is comparable to the drainage evolution described in other orogenic
608 belts such as the Moroccan High Atlas. The evolution from longitudinal to transverse
609 drainage in the Eastern Cordillera of Colombia may lead to a progressive area reduction
610 and eventually a disappearance of the high plateau of the Sabana de Bogotá.

611

612 **Acknowledgements**

613 This work was financed by Spanish MINECO project CGL2010-15416. L. Struth was
614 supported by an FPI PhD grant (BES-2011-050262) from MEC (Spain). We acknowledge
615 Andrés Mora, Andrés Valencia, Eliseo Tesón, and Maria Luisa Arboleya for assistance and
616 discussion during field work. Logistic support was generously provided by the ICP-
617 Ecopetrol. We thank the three reviewers of the manuscript for incisive and instructive
618 comments that helped to significantly improve the original text and figures.

619

620 **References**

- 621 Allen, P.A., 2008. From landscapes into geological history. *Nature*, 451, 274–276.
622 <http://doi.org/10.1038/nature06586>
- 623 Andriessen, P.A.M., Helmens, K.F., Hooghiemstra, H., Riezebos, P.A., Van der Hammen, T., 1993.
624 Absolute chronology of the Pliocene-Quaternary sediment sequence of the Bogota area,
625 Colombia. *Quaternary Science Reviews*, 12, 483–501. [http://doi.org/10.1016/0277-](http://doi.org/10.1016/0277-3791(93)90066-U)
626 [3791\(93\)90066-U](http://doi.org/10.1016/0277-3791(93)90066-U)
- 627 Antón, L., Rodés, A., De Vicente, G., Pallàs, R., Garcia-Castellanos, D., Stuart, F.M. Braucher, R.,
628 Bourlès, D., 2012. Quantification of fluvial incision in the Duero Basin (NW Iberia) from
629 longitudinal profile analysis and terrestrial cosmogenic nuclide concentrations.
630 *Geomorphology*, 165-166, 50–61. <http://doi.org/10.1016/j.geomorph.2011.12.036>
- 631 Babault, J., Van Den Driessche, J., Teixell, A., 2012. Longitudinal to transverse drainage network
632 evolution in the High Atlas (Morocco): The role of tectonics. *Tectonics*, 31.
633 <http://doi.org/10.1029/2011TC003015>
- 634 Babault, J., Teixell, A., Struth, L., Driessche, J. Van Den, Arbolea, M., Tesón, E., 2013. Shortening,
635 structural relief and drainage evolution in inverted rifts: insights from the Atlas Mountains,
636 the Eastern Cordillera of Colombia and the Pyrenees. *Geological Society of London, Special
637 Publications*, 377, 141–158. <http://doi.org/10.1144/SP377.14>
- 638 Bande, A., Horton, B.K., Ramírez, J.C., Mora, A., Parra, M., Stockli, D.F., 2012. Clastic deposition,
639 provenance, and sequence of Andean thrusting in the frontal Eastern Cordillera and Llanos
640 foreland basin of Colombia. *Bulletin of the Geological Society of America*, 124, 59–76.
641 <http://doi.org/10.1130/B30412.1>
- 642 Bayona, G., 2008. Geocronología, termocronología, bioestratigrafía y procedencia de unidades
643 paleógenas en la zona axial de la Cordillera Oriental; Aportes al modelamiento del sistema
644 petrolífero en las cuencas adyacentes. ICP-Ecopetrol report.
- 645 Bayona, G., Cortés, M., Jaramillo, C., Ojeda, G., Aristizabal, J.J., Reyes-Harker, A., 2008. An
646 integrated analysis of an orogen-sedimentary basin pair: Latest Cretaceous-Cenozoic
647 evolution of the linked Eastern Cordillera orogen and the Llanos foreland basin of Colombia.
648 *Bulletin of the Geological Society of America*, 120, 1171–1197.
649 <http://doi.org/10.1130/B26187.1>
- 650 Bishop, P., 1995. Drainage rearrangement by river capture, beheading and diversion. *Progress in
651 Physical Geography*, 19, 449–473. <http://doi.org/10.1177/030913339501900402>
- 652 Bonnet, S., 2009. Shrinking and splitting of drainage basins in orogenic landscapes from the
653 migration of the main drainage divide. *Nature Geoscience*, 2, 766–771.
654 <http://doi.org/10.1038/ngeo666>
- 655 Bookhagen, B., Burbank, D.W., 2010. Toward a complete Himalayan hydrological budget:
656 Spatiotemporal distribution of snowmelt and rainfall and their impact on river discharge.
657 *Journal of Geophysical Research: Earth Surface*, 115, 1–25.
658 <http://doi.org/10.1029/2009JF001426>

- 659 Bookhagen, B., Strecker, M. R., 2008. Orographic barriers, high-resolution TRMM rainfall, and relief
660 variations along the eastern Andes. *Geophysical Research Letters*, 35, 1–6.
661 <http://doi.org/10.1029/2007GL032011>
- 662 Brocard, G., Willenbring, J., Suski, B., Audra, P., Authemayou, C., Cosenza-Murales, B., Moran-Ical,
663 S., Demory, F., Rochette, P., Vennemann, T., Holliger, K., Teyssier, C., 2012. Rate and
664 processes of river network rearrangement during incipient faulting: The case of the Cahabon
665 River, Guatemala. *American Journal of Science*, 312, 449–507.
666 <http://doi.org/10.2475/05.2012.01>
- 667 Brocklehurst, S.H., Whipple, K.X., 2002. Glacial erosion and relief production in the Eastern Sierra
668 Nevada, California. *Geomorphology*, 42, 1–24. [http://doi.org/10.1016/S0169-555X\(01\)00069-](http://doi.org/10.1016/S0169-555X(01)00069-1)
669 1
- 670 Brookfield, M.E., 1998. Evolution of the great river systems of southern Asia during the Cenozoic
671 India-Asia collision: Rivers draining southwards. *Geomorphology*, 22, 285–312.
672 <http://doi.org/10.1016/j.geomorph.2008.01.003>
- 673 Brown, E.T., Edmond, J.M., Raisbeck, G.M., Yiou, F., Kurz, M.D., Brook, E.J., 1991. Examination of
674 surface exposure ages of Antarctic moraines using in situ produced ¹⁰Be and ²⁶Al.
675 *Geochimica et Cosmochimica Acta*. [http://doi.org/10.1016/0016-7037\(91\)90103-C](http://doi.org/10.1016/0016-7037(91)90103-C)
- 676 Bull, W.B., 1991. *Geomorphic Responses to Climatic Change*. Oxford University Press: New York.
- 677 Caballero, V., Mora, A., Quintero, I., Blanco, V., Parra, M., Rojas, L.E., Lopez, C., Sanchez, N., Horton,
678 B.K. Stockli, S., Duddy, I., 2013. Tectonic controls on sedimentation in an intermontane
679 hinterland basin adjacent to inversion structures: the Nuevo Mundo syncline, Middle
680 Magdalena Valley, Colombia. *Geological Society, London, Special Publications*, 377, 315–342.
681 <http://doi.org/10.1144/SP377.12>
- 682 Castellort, S., Goren, L., Willett, S.D., Champagnac, J.D., Herman, F., Braun, J., 2012. River drainage
683 patterns in the New Zealand Alps primarily controlled by plate tectonic strain. *Nature*
684 *Geoscience*, 5, 744–748. <http://doi.org/10.1038/ngeo1582>
- 685 Champel, B., 2002. Growth and lateral propagation of fault-related folds in the Siwaliks of western
686 Nepal: Rates, mechanisms, and geomorphic signature. *Journal of Geophysical Research*, 107.
687 <http://doi.org/10.1029/2001JB000578>
- 688 Clark, M.K., Schoenbohm, L.M., Royden, L.H., Whipple, K.X., Burchfiel, B.C., Zhang, X., Tang, W.,
689 Wang, E., Chen, L., 2004. Surface uplift, tectonics, and erosion of eastern Tibet from large-
690 scale drainage patterns. *Tectonics*, 23, TX1006. doi:10.1029/2002TC001402
- 691 Colletta, B., Hebrard, F., Letouzey, J., Werner, P., Rudkiewicz, J.R., 1990. Tectonic style and crustal
692 structure of the Eastern Cordillera (Colombia) from a balanced cross-section. *Petroleum and*
693 *Tectonics in Mobile Belts*, 81–100.
- 694 Cooper, M.A, Addison, F.T., Alvares, R., Hayward, A.B., Howe, S., Pulham, A.J., Taborda, A., 1995.
695 Basin development and tectonic history of the Llanos basin, Colombia. *Petroleum Basins of*
696 *South America*. AAPG. Memoir No. 62, 10, 659–666.

- 697 Cortés, M., Colletta, B., Angelier, J., 2006. Structure and tectonics of the central segment of the
698 Eastern Cordillera of Colombia. *Journal of South American Earth Sciences*, 21, 437–465.
699 <http://doi.org/10.1016/j.jsames.2006.07.004>
- 700 Dengo, C.A., Covey, M.C., 1993. Structure of the Eastern Cordillera of Colombia: Implications for
701 trap styles and regional tectonics. *American Association of Petroleum Geologists Bulletin*, 77,
702 1315–1337.
- 703 Diaz, L., Serrano, M., 2001. Observaciones sobre el Terciario del Piedemonte. Reporte Presentado a
704 Occidental de Colombia Por Ariana Ltda.
- 705 DiBiase, R.A., Whipple, K.X., Heimsath, A. M., Ouimet, W.B., 2010. Landscape form and millennial
706 erosion rates in the San Gabriel Mountains , CA. *Earth and Planetary Science Letters*, 289,
707 134–144. <http://doi.org/10.1016/j.epsl.2009.10.036>
- 708 Duque-Caro, H., 1990. Neogene stratigraphy, paleoceanography and paleobiogeography in
709 northwest South America and the evolution of the Panama Seaway. *Palaeo*, 77, 203–234.
- 710 Gómez, E., Jordan, T.E., Allmendinger, R.W., Hegarty, K., Kelley, S., Heizler, M., 2003. Controls on
711 architecture of the Late Cretaceous to Cenozoic southern Middle Magdalena Valley Basin,
712 Colombia. *GSA Bulletin*, 131–147. [http://doi.org/10.1130/0016-](http://doi.org/10.1130/0016-7606(2003)115<0131:COAOTL>2.0.CO;2)
713 [7606\(2003\)115<0131:COAOTL>2.0.CO;2](http://doi.org/10.1130/0016-7606(2003)115<0131:COAOTL>2.0.CO;2)
- 714 Gómez, E., Jordan, T.E., Allmendinger, R.W., Cardozo, N., 2005a. Development of the Colombian
715 foreland-basin system as a consequence of diachronous exhumation of the northern Andes.
716 *Geological Society of America Bulletin*, 117, 1272. <http://doi.org/10.1130/B25456.1>
- 717 Gómez, E., Jordan, T.E., Allmendinger, R.W., Cardozo, N., 2005b. Development of the Colombian
718 foreland-basin system as a consequence of diachronous exhumation of the northern Andes.
719 *Bulletin of the Geological Society of America*, 117, 1272–1292.
720 <http://doi.org/10.1130/B25456.1>
- 721 Gómez, E., Jordan, T.E., Allmendinger, R.W., Hegarty, K., Kelley, S., 2005c. Syntectonic Cenozoic
722 sedimentation in the northern middle Magdalena Valley Basin of Colombia and implications
723 for exhumation of the Northern Andes. *Bulletin of the Geological Society of America*, 117,
724 547–569. <http://doi.org/10.1130/B25454.1>
- 725 Goren, L., Fox, M., Willett, S.D., 2014. Tectonics from fluvial topography using formal linear
726 inversion: Theory and applications to the Inyo Mountains, California. *Journal of Geophysical*
727 *Research: Earth Surface*, n/a–n/a. <http://doi.org/10.1002/2014JF003079>
- 728 Gregory-Wodzicki, K.M., 2000. Uplift history of the Central and Northern Andes: A review.
729 *Geological Society of America Bulletin*, 112, 1091–1105. [http://doi.org/10.1130/0016-](http://doi.org/10.1130/0016-7606(2000)112<1091:uhotca>2.0.co;2)
730 [7606\(2000\)112<1091:uhotca>2.0.co;2](http://doi.org/10.1130/0016-7606(2000)112<1091:uhotca>2.0.co;2)
- 731 Gupta, S., 1997. Himalayan drainage patterns and the origin of fluvial megafans in the Ganges
732 foreland basin. *Geology*, 25, 11–14.

- 733 Helmens, K.F., 1988. Late Pleistocene glacial sequence in the area of the high plain of Bogotá
734 (Eastern Cordillera, Colombia). *Palaeogeogr. Palaeoclimatol. Palaeoecol.* 67, 263–283.
- 735 Helmens, K.F., 1990. Neogene-Quaternary Geology in the high plain of Bogotá, Eastern Cordillera,
736 Colombia (stratigraphy, paleoenvironments and landscape evolution). *Dissertas Botanicae*,
737 163, pp 202.
- 738 Helmens, K.F., 2004. The Quaternary glacial record of the Colombian Andes. In: Ehlers, J; Gibbard P
739 L (eds), *Quaternary Glaciations-extent and chronology, Part III: South America, Asia, Africa,*
740 *Australasia, Antarctica. Developments in Quaternary Science, 2c*, 115–134.
- 741 Helmens, K.F., Kuhry, P., 1995. Glacier fluctuations and vegetation change associated with Late
742 Quaternary climatic oscillations in the area of Bogotá, Colombia. *Quat. South America*
743 *Antarctica Peninsula*, 9, 117–140.
- 744 Helmens, K.F., Rutter, N.W., Kuhry, P., 1997. Glacier fluctuations in the eastern Andes of Colombia
745 (South America) during the past 45,000 radiocarbon years. *Quaternary International* 38-9,
746 39–48.
- 747 Hermeston, S., Nemcok, M., 2013. Thick-skin orogen-foreland interactions and their controlling
748 factors, Northern Andes of Colombia. *Geological Society, London, Special Publications*, 377,
749 443–471. <http://doi.org/10.1144/SP377.16>
- 750 Hooghiemstra, H., Wijninga, V.M., Cleef, A.M., 2006. The paleobotanical record of Colombia:
751 implications for biogeography and biodiversity. *Annals of Missouri Botanical Garden*, 93,
752 297–325.
- 753 Hoorn, C., Guerrero, J., Sarmiento, G.A., Lorente, M.A., 1995. Andean tectonics as a cause for
754 changing drainage patterns in Miocene northern South America. *Geology*, 23, 237–240.
755 [http://doi.org/10.1130/0091-7613\(1995\)023<0237:ATAACF>2.3.CO;2](http://doi.org/10.1130/0091-7613(1995)023<0237:ATAACF>2.3.CO;2)
- 756 Horton, B.K., Saylor, J.E., Nie, J., Mora, A., Parra, M., Reyes-Harker, A., Stockli, D.F., 2010. Linking
757 sedimentation in the northern Andes to basement configuration, Mesozoic extension, and
758 Cenozoic shortening: Evidence from detrital zircon U-Pb ages, Eastern Cordillera, Colombia.
759 *Bulletin of the Geological Society of America*, 122, 1423–1442.
760 <http://doi.org/10.1130/B30118.1>
- 761 Howard, A.D., Kerby, G., 1983. Channel changes in badlands. *Geological Society of America Bulletin*,
762 94, 739-752.
- 763 Humphrey, N.F., Konrad, S.K., 2000. River incision or diversion in response to bedrock uplift.
764 *Geology*, 28, 43–46. [http://doi.org/10.1130/0091-7613\(2000\)028<0043:RIODIR>2.3.CO;2](http://doi.org/10.1130/0091-7613(2000)028<0043:RIODIR>2.3.CO;2)
- 765 Jarvis, A., Reuter, H.I., Nelson, A., Guevara, E., 2008. Hole-filled SRTM for the globe. Version 4.
766 <http://srtm.csi.cgiar.org>.
- 767 Jimenez, L., Mora, A., Casallas, W., Silva, A., Teson, E., Tamara, J., Namson, J., Higuera-Diaz, I.C.,
768 Lasso, A., Stockli, D., 2013. Segmentation and growth of foothill thrust-belts adjacent to

- 769 inverted grabens: the case of the Colombian Llanos foothills. Geological Society, London,
770 Special Publications, 377, 189–220. <http://doi.org/10.1144/SP377.11>
- 771 Julivert, M., 1963. Los rasgos tectónicos de la región de la Sabana de Bogotá y los mecanismos de la
772 formación de las estructuras. Boletín de Geología Universidad Industrial Santander, 13-14, 5–
773 102.
- 774 Julivert, M., 1970. Cover and Basement Tectonics in the Cordillera Oriental of Colombia, South
775 America, and a Comparison with Some Other Folded Chains. Geological Society of America
776 Bulletin, 81, 3623–3646.
- 777 Kellogg, J.N., Vega, V., 1995. Tectonic development of Panama, Costa Rica, and the Colombian
778 Andes: Constraints from global positioning system geodetic studies and gravity. Geologic and
779 Tectonic Development of the Caribbean Plate Boundary in Southern Central America.
780 <http://doi.org/10.1130/SPE295-p75>
- 781 Kirby, E., 2003. Distribution of active rock uplift along the eastern margin of the Tibetan Plateau:
782 Inferences from bedrock channel longitudinal profiles. Journal of Geophysical Research, 108,
783 2217. <http://doi.org/10.1029/2001JB000861>
- 784 Kirby, E., Whipple, K., 2001. Quantifying differential rock-uplift rates via stream profile analysis.
785 Geology, 6, 415–418.
- 786 Kooi, H., Beaumont, C., 1996. Large-scale geomorphology: Classical concepts reconciled and
787 integrated with contemporary ideas via a surface processes model. Journal of Geophysical
788 Research, 101, 3361. <http://doi.org/10.1029/95JB01861>
- 789 Koons, P. O., 1994. Three-dimensional critical wedges: Tectonics and topography in oblique
790 collisional orogens. Journal of Geophysical Research, 99, 12301–12315.
791 <http://doi.org/10.1029/94JB00611>
- 792 Koons, P.O., 1995. Modeling the topographic evolution of collisional belts. Annual Review of Earth
793 and Planetary Sciences, 23, 375–408.
- 794 Laverde, F.E., Segall, M.P., Allen, R.B., Resselar, R., 1989. Recognition of an ancient fluvial system in
795 the Upper Magdalena Valley, Colombia. In Programme and Abstracts of the IV International
796 Conference on Fluvial Sedimentology (Barcelona), p. 165.
- 797 Mark, B.G., Helmens, K.F., 2005. Reconstruction of glacier equilibrium-line altitudes for the Last
798 Glacial Maximum on the High Plain of Bogota, Eastern Cordillera, Colombia: Climatic and
799 topographic implications. J. Quat. Sci. 20, 789–800. doi:10.1002/jqs.974
- 800 Mather, A. E., 2000. Adjustment of a drainage network to capture induced base-level change: an
801 example from the Sorbas Basin, SE Spain. Geomorphology, 34, 271–289.
802 [http://doi.org/10.1016/S0169-555X\(00\)00013-1](http://doi.org/10.1016/S0169-555X(00)00013-1)
- 803 Molnar, P., England, P., 1990. Late Cenozoic uplift of mountain ranges and global climatic change:
804 chicken or egg? Nature, 346, 29–34.

- 805 Mora, A., Parra, M., Strecker, M.R., Kammer, A., Dimaté, C., Rodríguez, F., 2006. Cenozoic
806 contractional reactivation of Mesozoic extensional structures in the Eastern Cordillera of
807 Colombia. *Tectonics*, 25, 1–19. <http://doi.org/10.1029/2005TC001854>
- 808 Mora, A., Parra, M., Strecker, M.R., Sobel, E.R., Hooghiemstra, H., Torres, V., Jaramillo, J. V., 2008.
809 Climatic forcing of asymmetric orogenic evolution in the Eastern Cordillera of Colombia.
810 *Bulletin of the Geological Society of America*, 120, 930–949.
811 <http://doi.org/10.1130/B26186.1>
- 812 Mora, A., Horton, B.K., Mesa, A., Rubiano, J., Ketcham, R.A., Parra, M., Blanco, V., Garcia, D., Stockli,
813 D.F., 2010. Migration of cenozoic deformation in the eastern cordillera of colombia
814 interpreted from fission track results and structural relationships: Implications for petroleum
815 systems. *AAPG Bulletin*, 94, 1543–1580. <http://doi.org/10.1306/01051009111>
- 816 Mora, A., Reyes-Harker, A., Rodriguez, G., Teson, E., Ramirez-Arias, J.C., Parra, M., Caballero, V.,
817 Mora, J.P., Quintero, I., Valencia, V., Ibanez, M., Horton, B.K, Stockli, D. F., 2013. Inversion
818 tectonics under increasing rates of shortening and sedimentation: Cenozoic example from
819 the Eastern Cordillera of Colombia. *Geological Society, London, Special Publications*, 377,
820 411–442. <http://doi.org/10.1144/SP377.6>
- 821 Moreno, N., Silva, A., Mora, A., Tesón, E., Quintero, I., Rojas, L.E., Lopez, C., Blanco, V., Castellanos,
822 J., Sanchez, J., Osorio, L., Namson, J., Stockli, D., Casallas, W., 2013. Interaction between thin-
823 and-thick-skinned tectonics in the foothill areas of an inverted graben. *The Middle*
824 *Magdalena Foothill belt. Geol. Soc. London, Spec. Publ.* 377, 221-255. [Doi:10.1144/SP377.18](http://doi.org/10.1144/SP377.18)
- 825 Mudd, S.M., Attal, M., Milodowski, D.T., Grieve, S.W.D., Valters, D.A., 2014. A statistical framework
826 to quantify spatial variation in channel gradients using the integral method of channel profile
827 analysis. *Journal of Geophysical Research: Earth Surface*, 119, 138–152.
828 <http://doi.org/10.1002/2013JF002981>
- 829 Nie, J., Horton, B.K., Mora, A., Saylor, J.E., Housh, T.B., Rubiano, J., Naranjo, J., 2010. Tracking
830 exhumation of Andean ranges bounding the Middle Magdalena Valley Basin, Colombia.
831 *Geology*, 38, 451–454. <http://doi.org/10.1130/G30775.1>
- 832 Nie, J., Horton, B.K., Saylor, J.E., Mora, A., Mange, M., Garziona, C.N., Basu, A., Moreno, C.J.,
833 Caballero, V., Parra, M., 2012. Integrated provenance analysis of a convergent retroarc
834 foreland system: U-Pb ages, heavy minerals, Nd isotopes, and sandstone compositions of the
835 Middle Magdalena Valley basin, northern Andes, Colombia. *Earth-Science Reviews*, 110, 111–
836 126. <http://doi.org/10.1016/j.earscirev.2011.11.002>
- 837 O’Callaghan, J.F., Mark, D.M., 1984. The extraction of drainage networks from digital elevation
838 data. *Computer Vision, Graphics, and Image Processing*, 28, 323–344.
- 839 Parra, M., Mora, A., Jaramillo, C., Strecker, M.R., Sobel, E.R., Quiroz, L., Rueda, M., Torres, V.,
840 2009a. Orogenic wedge advance in the northern Andes: Evidence from the Oligocene-
841 Miocene sedimentary record of the Medina Basin, Eastern Cordillera, Colombia. *Bulletin of*
842 *the Geological Society of America*, 121, 780–800. <http://doi.org/10.1130/B26257.1>

- 843 Parra, M., Mora, A., Sobel, E.R., Strecker, M.R., González, R., 2009b. Episodic orogenic front
844 migration in the northern Andes: Constraints from low-temperature thermochronology in the
845 Eastern Cordillera, Colombia. *Tectonics*, 28. <http://doi.org/10.1029/2008TC002423>
- 846 Parra, M., Mora, A., Jaramillo, C., Torres, V., Zeilinger, G., Strecker, M.R., 2010. Tectonic controls on
847 Cenozoic foreland basin development in the north-eastern Andes, Colombia. *Basin Research*,
848 22, 874–903. <http://doi.org/10.1111/j.1365-2117.2009.00459.x>
- 849 Pelletier, J.D., 2004. Persistent drainage migration in a numerical landscape evolution model.
850 *Geophysical Research Letters*, 31, L20501. <http://doi.org/10.1029/2004GL020802>
- 851 Perron, J.T., Royden, L., 2013. An integral approach to bedrock river profile analysis. *Earth Surface*
852 *Processes and Landforms*, 38, 570–576. <http://doi.org/10.1002/esp.3302>
- 853 Perron, J.T., Richardson, P.W., Ferrier, K.L., Lapôtre, M., 2012. The root of branching river networks.
854 *Nature*, 492, 100–103. <http://doi.org/10.1038/nature11672>
- 855 Prince, P.S., Spotila, J.A., Henika, W.S., 2011. Stream capture as driver of transient landscape
856 evolution in a tectonically quiescent setting. *Geology*, 39, 823–826.
857 <http://doi.org/10.1130/G32008.1>
- 858 Restrepo-Pace, P.A., Colmenares, F., Higuera, C., Mayorga, M., 2004. A Fold-and-thrust belt along
859 the western flank of the Eastern Cordillera of Colombia—Style, kinematics, and timing
860 constraints derived from seismic data and detailed surface mapping. *Thrust Tectonics and*
861 *Hydrocarbon Systems*, 598–613.
- 862 Roeder, D., Chamberlain, R.L., 1995. Eastern Cordillera of Colombia: Jurassic–Neogene crustal
863 evolution. In A. J. Tankard, S. R. Suarez, and H. J. Welsink, Eds., *Petroleum Basins of*
864 *South America: AAPG Memoir* 62, 633–645.
- 865 Rolon, L.F., Toro, J., Wilson, T., 2004. Structural Geometry of the Jura-Cretaceous Rift of the Middle
866 Magdalena Valley Basin – Colombia.
- 867 Royden, L., Perron, J.T., 2013. Solutions of the stream power equation and application to the
868 evolution of river longitudinal profiles. *Journal of Geophysical Research: Earth Surface*, 118,
869 497–518. <http://doi.org/10.1002/jgrf.20031>
- 870 Safran, E.B., Bierman, P.R., Aalto, R., Dunne, T., Whipple, K.X., Caffee, M., 2005. Erosion rates driven
871 by channel network incision in the Bolivian Andes. *Earth Surface Processes and Landforms*,
872 30, 1007–1024. <http://doi.org/10.1002/esp.1259>
- 873 Saylor, J.E., Horton, B. K., Nie, J., Corredor, J., Mora, A., 2011. Evaluating foreland basin partitioning
874 in the northern Andes using Cenozoic fill of the Floresta basin, Eastern Cordillera, Colombia.
875 *Basin Research*, 23, 377–402. <http://doi.org/10.1111/j.1365-2117.2010.00493.x>
- 876 Schumm, S.A., 1979. Geomorphic Thresholds: the concept and its application. *Transaction of the*
877 *Institute of British Geographers*, 4, 485–515.
- 878 Silva, A., Mora, A., Caballero, V., Rodriguez, G., Ruiz, C., Moreno, N., Parra, M., Ramirez-Arias, J.C.,
879 Ibanez, M., Quintero, I., 2013. Basin compartmentalization and drainage evolution during rift

- 880 inversion: evidence from the Eastern Cordillera of Colombia. Geological Society, London,
881 Special Publications, 377, 369–409. <http://doi.org/10.1144/SP377.15>
- 882 Small, R.J., 1978. The study of landforms (2nd edn). Cambridge: Cambridge University Press.
- 883 Snyder, N.P., Whipple, K.X., Tucker, G.E., Merritts, D.J., 2003. Channel response to tectonic forcing:
884 field analysis of stream morphology and hydrology in the Mendocino triple junction region,
885 northern California. *Geomorphology*, 53, 97–127. [http://doi.org/10.1016/S0169-](http://doi.org/10.1016/S0169-555X(02)00349-5)
886 [555X\(02\)00349-5](http://doi.org/10.1016/S0169-555X(02)00349-5)
- 887 Sobel, E.R., Hilley, G.E., Strecker, M.R., 2003. Formation of internally drained contractional basins
888 by aridity-limited bedrock incision. *Journal of Geophysical Research: Solid Earth*, 108.
889 <http://doi.org/10.1029/2002JB001883>
- 890 Stokes, M., Mather, A.E., Harvey, A.M., 2002. Quantification of river-capture-induced base-level
891 changes and landscape development, Sorbas Basin, SE Spain. Geological Society, London,
892 Special Publications, 191, 23–35. <http://doi.org/10.1144/GSL.SP.2002.191.01.03>
- 893 Taboada, A., Rivera, L.A., Fuenzalida, A., Cisternas, A., Philip, H., Bijwaard, H., Olaya, J., Rivera, C.,
894 2000. Geodynamics of the northern Andes: Subductions and intracontinental deformation
895 (Colombia). *Tectonics*, 19, 787–813. <http://doi.org/10.1029/2000TC900004>
- 896 Tarboton, D. G., 1997. A new method of determination of flow directions and upslope areas in grid
897 digital elevation models. *Water Resources Research*, 33, 309–319.
- 898 Teixell, A., Tesón, E., Ruiz, J.C., Mora, A., 2015. The structure of an inverted back-arc rift : insights
899 from a transect across the Eastern Cordillera of Colombia near Bogotá. , in C. Bartolini, and P.
900 Mann, eds. *Petroleum Geology and Hydrocarbon Potential of Colombia Caribbean Margin:*
901 *AAPG Memoir*, 108, in press.
- 902 Tesón, E., Mora, A., Silva, A., Namson, J., Teixell, A., Castellanos, J., Casallas, W., Julivert, M., Taylor,
903 M., Ibanez-Mejia, M., Valencia, V.A., 2013. Relationship of Mesozoic graben development,
904 stress, shortening magnitude, and structural style in the Eastern Cordillera of the Colombian
905 Andes. Geological Society, London, Special Publications, 377, 257–283.
906 <http://doi.org/10.1144/SP377.10>
- 907 Tomkin, J. H., Braun, J., 1999. Simple models of drainage reorganisation on a tectonically active
908 ridge system. *New Zealand Journal of Geology & Geophysics*, 42, 1–10.
- 909 Toro, J., Roure, Bordas-Le Floch, N., Le Cornec-Lance, S., Sassi, W., 2004. Thermal and Kinematic
910 Evolution of the Eastern Cordillera Fold and Thrust Belt, Colombia. *Am. Assoc. Pet. Geol.* 1,
911 79-115. Doi:10.1306/1025687H13114
- 912 Torres, V., Vandenberghe, J., Hooghiemstra, H., 2005. An environmental reconstruction of the
913 sediment infill of the Bogotá basin (Colombia) during the last 3 million years from abiotic and
914 biotic proxies. *Palaeogeography, Palaeoclimatology, Palaeoecology*, 226, 127–148.
915 <http://doi.org/10.1016/j.palaeo.2005.05.005>

- 916 Van der Beek, P., Champel, B., Mugnier, J.L., 2002. Control of detachment dip on drainage
917 development in regions of active fault-propagation folding. *Geology*, 30, 471–474.
918 [http://doi.org/10.1130/0091-7613\(2002\)030<0471:CODDOD>2.0.CO;2](http://doi.org/10.1130/0091-7613(2002)030<0471:CODDOD>2.0.CO;2)
- 919 Van der Hammen, T., Werner, J.H., van Dommelen, H., 1973. Palynological record of the upheaval
920 of the Northern Andes: A study of the pliocene and lower quaternary of the Colombian
921 Eastern Cordillera and the early evolution of its high-Andean biota. *Review of Palaeobotany
922 and Palynology*, 16, 1–122. [http://doi.org/10.1016/0034-6667\(73\)90031-6](http://doi.org/10.1016/0034-6667(73)90031-6)
- 923 Veloza, G., Taylor, M., Mora, A., Gosse, J., 2015. Active mountain building along the eastern
924 Colombian Subandes: A folding history from deformed terraces across the Tame anticline,
925 Llanos Basin. *Geological Society of America Bulletin*, 1–19. <http://doi.org/10.1130/B31168.1>
- 926 Whitfield, E., Harvey, A.M., 2012. Interaction between the controls on fluvial system development:
927 Tectonics, climate, base level and river capture - Rio Alias, Southeast Spain. *Earth Surface
928 Processes and Landforms*, 37, 1387–1397. <http://doi.org/10.1002/esp.3247>
- 929 Willett, S.D., 1999. Orogeny and orography: The effects of erosion on the structure of mountain
930 belts. *Journal of Geophysical Research*, 104, 28957. <http://doi.org/10.1029/1999JB900248>
- 931 Willett, S.D., Slingerland, R., Hovius, N., 2001. Uplift, shortening, and steady state topography in
932 active mountain belts. *Am. J. Sci.*, 301, 455–485
- 933 Willett, S.D., McCoy, S.W., Perron, J.T., Goren, L., Chen, C.-Y., 2014. Dynamic reorganization of river
934 basins. *Science (New York, N.Y.)*, 343, 1248765. <http://doi.org/10.1126/science.1248765>
- 935 Wobus, C., Whipple, K.X., Snyder, N., Johnson, J., Sheehan, D., 2006. Tectonics from topography :
936 Procedures , promise , and pitfalls, 2398, 55–74. [http://doi.org/10.1130/2006.2398\(04\)](http://doi.org/10.1130/2006.2398(04))
- 937
- 938
- 939